nature immunology

The NLRP3 inflammasome is released as a particulate danger signal that amplifies the inflammatory response

Alberto Baroja-Mazo[1,8], Fatima Martín-Sánchez[1,8], Ana I Gomez[1], Carlos M Martínez[1], Joaquín Amores-Iniesta[1], Vincent Compan[2,7], Maria Barberà-Cremades[1], Jordi Yagüe[3], Estibaliz Ruiz-Ortiz[3], Jordi Antón[4], Segundo Buján[5], Isabelle Couillin[6], David Brough[2], Juan I Arostegui[3] & Pablo Pelegrín[1,2]

Assembly of the NLRP3 inflammasome activates caspase-1 and mediates the processing and release of the leaderless cytokine IL-1β and thereby serves a central role in the inflammatory response and in diverse human diseases. Here we found that upon activation of caspase-1, oligomeric NLRP3 inflammasome particles were released from macrophages. Recombinant oligomeric protein particles composed of the adaptor ASC or the p.D303N mutant form of NLRP3 associated with cryopyrin-associated periodic syndromes (CAPS) stimulated further activation of caspase-1 extracellularly, as well as intracellularly after phagocytosis by surrounding macrophages. We found oligomeric ASC particles in the serum of patients with active CAPS but not in that of patients with other inherited autoinflammatory diseases. Our findings support a model whereby the NLRP3 inflammasome, acting as an extracellular oligomeric complex, amplifies the inflammatory response.

Inflammation is a tightly regulated response of the innate immune system to infection and tissue injury and aims to restore tissue homeostasis. Several soluble cytokines have crucial roles in this process, including various inflammatory interleukins that lack a signal peptide, such as interleukin 1β (IL-1β) or IL-18 (ref. 1). Both of those cytokines are synthesized as inactive precursors and require post-translational processing by active caspase-1 for the generation of their mature active forms[1]. The activation of caspase-1 is driven by the assembly of cytosolic multiprotein complexes called 'inflammasomes'. Inflammasome complexes are composed of a sensor protein connected to caspase-1, an interaction that in most cases requires the adaptor ASC ('apoptosis-associated Speck-like protein with a caspase-recruitment domain'; encoded by *Pycard*)[2]. Inflammasome-dependent activation of caspase-1 is also required for the poorly understood unconventional release of IL-1β and IL-18 (ref. 3). Deregulated production of IL-1β underlies various human inflammatory diseases, including the inherited cryopyrin-associated periodic syndromes (CAPS), gout, atherosclerosis and type 2 diabetes[4–7].

The NLRP3 inflammasome is the most extensively studied inflammasome that is formed after the oligomerization of NLRP3 and subsequent recruitment of ASC and pro-caspase-1 (ref. 2). Upon activation of NLRP3, ASC proteins assemble into fiber-like structures; this culminates in the production of a large protein aggregate that enormously amplifies the activation of caspase-1 (refs. 8,9). The NLRP3 inflammasome is activated in response to a variety of infectious stimuli or to cellular stress caused by various sterile danger signals[2], including high concentrations of extracellular ATP, a decrease in extracellular osmolarity or pH, crystals of monosodium urate or cholesterol, β-amyloid fibers, the degradation of extracellular matrix components, vaccine adjuvants, and environmental or industrial particles and nanoparticles[6,7,10–16]. All those extracellular stimuli converge to activate the NLRP3 inflammasome through a mechanism that is undefined but has been suggested to include a decrease in the intracellular concentration of K^+, signaling via Ca^{2+}, the production of reactive oxygen species, damage to the phagolysosomal membrane, the activity of cathepsins, the release of oxidized mitochondrial DNA into the cytosol secondary to mitochondrial damage, activation of the kinase TAK1 and deubiquitination of NLRP3 (refs. 11,17–22).

In conjunction with the release of mature IL-1β and IL-18, the inflammasome-dependent activation of caspase-1 also controls the release of additional cytosolic proteins through an unconventional pathway that includes the release of alarmins such as HMGB1 (refs. 23,24). Most reports studying caspase-1 maturation after inflammasome assembly have found active forms of caspase-1 (the subunits p10 and p20) in cell supernatants[6,11,17–22,25,26]. Such data suggest that caspase-1 may regulate its own release. However, the (patho-)physiological role of extracellular caspase-1 and the inflammasome remains to be addressed.

Here we report that oligomeric particles of the NLRP3 and ASC inflammasome were released together with IL-1β and active caspase-1 subunits after activation of the inflammasome. Oligomeric particles of ASC activated caspase-1 not only extracellularly but also after internalization into

[1]Inflammation and Experimental Surgery Unit, CIBERehd, Institute for Bio-Health Research of Murcia, Clinical University Hospital Virgen de la Arrixaca, Murcia, Spain. [2]Faculty of Life Sciences, University of Manchester, Manchester, UK. [3]Department of Immunology-CDB, Hospital Clinic, Barcelona, Spain. [4]Reumathology Pediatric Unit, Hospital Sant Joan de Deu, Barcelona, Spain. [5]Department of Internal Medicine, Hospital Vall d'Hebron, Barcelona, Spain. [6]Experimental and Molecular Immunology and Neurogenetics, CNRS UMR 7355, University of Orleans, Orleans, France. [7]Present address: Department of Cell Biology, University of Geneva, Geneva, Switzerland. [8]These authors contributed equally to this work. Correspondence should be addressed to P.P. (pablo.pelegrin@ffis.es).

Received 1 April; accepted 9 May; published online 22 June 2014; doi:10.1038/ni.2919

wild-type, ASC-deficient (*Pycard*$^{-/-}$) or NLRP3-deficient (*Nlrp3*$^{-/-}$) macrophages and therefore functioned as danger signals that spread inflammatory signaling to surrounding macrophages. Similarly, mutations in *NLRP3* that cause human CAPS also resulted in the formation of oligomeric particles of NLRP3 that, after being released from the cell, became functional and were able to activate caspase-1 in both wild-type and *Nlrp3*$^{-/-}$ mouse macrophages. We found ASC oligomers in the serum of patients with active CAPS but not in patients with the inherited autoinflammatory syndromes familial Mediterranean fever or tumor-necrosis factor (TNF) receptor–associated periodic syndrome.

RESULTS

Inflammasome components are released after activation of NLRP3

The activation of caspase-1 by the NLRP3 inflammasome is associated with secretion of the leaderless cytokines IL-1β and IL-18 via an unconventional release pathway[3]. As expected, activation of the NLRP3 inflammasome by ATP or nigericin resulted in the release of not only mature IL-1β and caspase-1 p10 but also the inflammasome components NLRP3, ASC and pro-caspase-1 (p45) into macrophage supernatants (**Fig. 1a**). Quantification of released protein relative to the total amount of intracellular protein revealed that after activation of the NLRP3 inflammasome, the majority of pool of IL-1β, caspase-1 p10 and ASC (>50%) was in the supernatant (**Supplementary Fig. 1a**). However, less than 50% of pro-IL-1β, pro-caspase-1 (p45), NLRP3 or β-actin was extracellular (**Supplementary Fig. 1a**). Time-course experiments revealed that all inflammasome components (ASC, caspase-1, NLRP3 and IL-1β) were detectable in the cell supernatant after 15 min of stimulation of the NLRP3 inflammasome (**Fig. 1b**). Full immunoblot analysis of intracellular proteins, extracellular IL-1β and caspase-1 revealed that little of the mature IL-1β or p10 remained associated with cell lysates (**Supplementary Fig. 1b**). Densitometry of extracellular proteins during the time course of stimulation of the NLRP3 inflammasome demonstrated that the kinetics of the release of inflammasome components was similar for all components during the first 30 min, then the release of NLRP3 was delayed relative to that of IL-1β, caspase-1 p10 and ASC (**Fig. 1c**). Prolonged activation

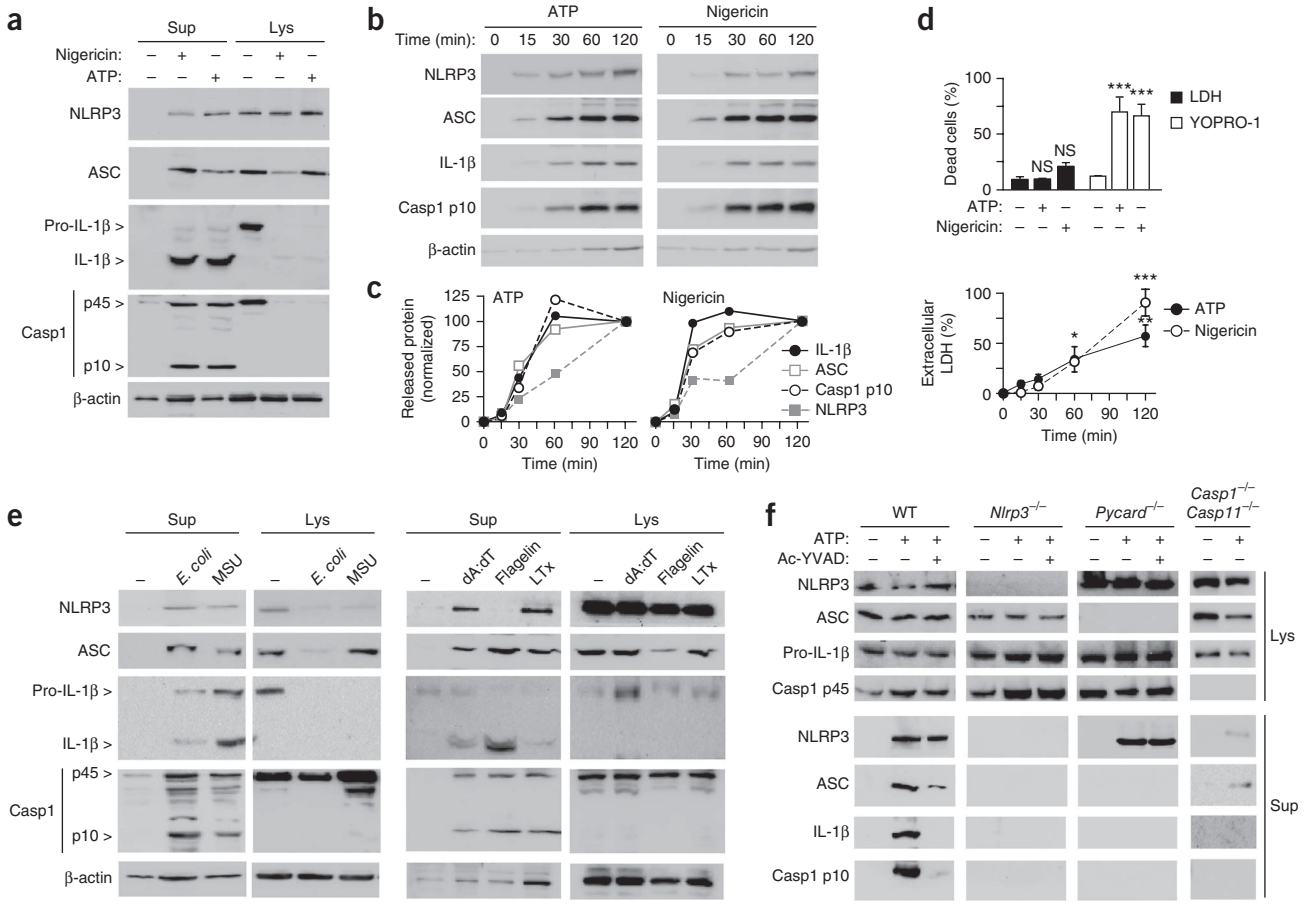

Figure 1 The activation of inflammasomes induces the release of NLRP3 and ASC. (**a**) Immunoblot analysis of inflammasome components in supernatants (Sup) and lysates (Lys) of mouse bone marrow–derived macrophages (BMDMs) primed for 4 h with LPS (1 μg/ml), followed by no stimulation (–) or stimulation (+) of NLRP3 for 30 min with nigericin (20 μM) or ATP (5 mM); β-actin serves as a loading control throughout. Casp1, caspase-1. (**b**) Immunoblot analysis of inflammasome components in cell-free supernatants of macrophages primed and stimulated for 0–120 min (above lanes) as in **a**. (**c**) Densitometry of proteins released from the cells in **b**, normalized to the release at 2 h after stimulation, set as 100. (**d**) Frequency of dead cells among macrophages treated as in **a**, assessed as extracellular LDH and permeabilization of the plasma membrane to YOPRO-1. (**e**) Immunoblot analysis of inflammasome components in supernatants and lysates of LPS-primed mouse BMDMs after no stimulation (–) or stimulation (for 16 h) of NLRP3 with *Escherichia coli* (*E. coli*; multiplicity of infection, 20) or monosodium urate crystals (MSU; 200 μg/ml), of AIM2 with poly(dA:dT) (dA:dT; 5 μg/ml), of NLRC4 with flagellin (100 ng/ml) or of NLRP1 with anthrax lethal toxin (LTx; 2.5 μg/ml). (**f**) Immunoblot analysis of inflammasome components in lysates and supernatants of wild-type (WT), *Nlrp3*$^{-/-}$, *Pycard*$^{-/-}$ and *Casp1*$^{-/-}$*Casp11*$^{-/-}$ BMDMs primed for 4 h with LPS (1 μg/ml) and then left unstimulated (–) or stimulated (+) for 30 min with ATP (5 mM) in the presence (+) or absence (–) of the caspase-1 inhibitor Ac-YVAD-AOM (Ac-YVAD; 50 μM). NS, not significant ($P > 0.05$); *$P < 0.05$, **$P < 0.01$ and ***$P < 0.001$, compared with unstimulated cells or time zero (Student's *t*-test). Data are representative of at least three independent experiments (**a**,**e**,**f**), two independent experiments (**b**,**c**) or five (top) or three (bottom) independent experiments (**d**; mean and s.e.m.).

of the inflammasome results in a specific type of cell death called 'pyroptosis', characterized by loss of plasma membrane integrity and the late release of intracellular proteins, including the cytosolic enzyme lactate dehydrogenase (LDH)[27]. To investigate whether the release of inflammasome components was associated with pyroptosis, we measured LDH in cell supernatants and the permeability of the plasma membrane to small molecules. Activation of NLRP3 for 30 min resulted in release of LDH below 25% of the total cellular LDH content, while the majority of cells presented a plasma membrane permeable to the plasma membrane–impermeant green fluorescent dye YOPRO-1 (molecular mass, 629 Da) (**Fig. 1d**). The release of LDH then increased over the period of stimulation and reached >50% of the total cellular LDH after 2 h of stimulation (**Fig. 1d**). This showed that upon activation of the NLRP3 inflammasome, NLRP3 and ASC were present extracellularly at early time points, together with the proinflammatory cytokine IL-1β.

We next found that activation of theNLRP3 inflammasome by particles, as well as activation of NLRP1 or AIM2 inflammasome, also led to the release of ASC, NLRP3, IL-1β and caspase-1 p10 (**Fig. 1e**). In contrast, activation of NLRC4 did not result in the release of NLRP3, but other inflammasome proteins were present extracellularly after such activation (**Fig. 1e**). Each of these treatments resulted in an increase in the release of LDH, from 25% to 50% of the total cellular content (**Supplementary Fig. 1c**).

Upon activation of the inflammasome, the release of NLRP3 was maintained after the inhibition of caspase-1, and the release of NLRP3 from *Pycard*$^{-/-}$ macrophages and macrophages doubly deficient in both caspase-1 and caspase-11 (*Casp1*$^{-/-}$*Casp4*$^{-/-}$; called '*Casp1*$^{-/-}$*Casp11*$^{-/-}$' here) was also maintained (**Fig. 1f** and **Supplementary Fig. 1f**). Quantification of the released protein by densitometry showed that when caspase-1 was inhibited, the release of NLRP3 was 16.3% less and that of ASC was 88.3% less than without such inhibition (**Supplementary Fig. 1d**). Activation of *Nlrp3*$^{-/-}$, *Pycard*$^{-/-}$ and *Casp1*$^{-/-}$*Casp11*$^{-/-}$macrophages by ATP did not result in a significant change in the release of LDH ($P > 0.05$; **Supplementary Fig. 1e**). All these data suggested that the majority of NLRP3 was passively released after sustained stimulation, whereas ASC release occurred quickly and was very much dependent on the activity of caspase-1.

Extracellular inflammasomes are oligomeric particles

We found that after 10–30 min of activation of the NLRP3 inflammasome, extracellular ASC was oligomeric, as revealed by experiments in which we crosslinked ASC with the succinimidyl-ester diazirine reagent SDA (**Fig. 2a** and **Supplementary Fig. 2a**). Extracellular ASC from macrophages activated by ATP immunoprecipitated together with NLRP3 (**Fig. 2b**), which suggested that NLRP3 and ASC were able to form oligomeric inflammasome particles extracellularly. By time-lapse microscopy of macrophages expressing ASC tagged with the red fluorescent protein mCherry (ASC-mCherry) and treated with nigericin, we found that following oligomerization of intracellular ASC, ASC specks were released after 5 min (**Supplementary Video 1**). We also detected extracellular ASC specks by immunofluorescence staining of ASC in macrophages activated with ATP (**Fig. 2c**). In these preparations, staining of the cell membrane with cholera toxin B and staining of the F-actin cytoskeleton with phalloidin revealed that some ASC specks were beyond the limit of the cell boundary (**Supplementary Fig. 2b**), which demonstrated that particulate ASC specks were present outside the cells. We then quantified ASC specks that were intracellular, near the inner cell surface or outside the cell (**Fig. 2d**) and found that after 20 min of stimulation with ATP, most of the ASC specks were extracellular (58% ± 15.5% (mean s.e.m.)) or near the cell perimeter (24% ± 12.8%) (**Fig. 2e**). Flow cytometry of cell-free supernatants of ATP-treated macrophages revealed extracellular inflammasome particles that stained positively for ASC and NLRP3 (**Fig. 2f**). These particles seemed to be close in size to that of calibrated beads 3 μm in diameter, as determined by flow cytometry (**Supplementary Fig. 2c**); however, we cannot exclude the possibility that particle aggregation occurred during sample preparation. We confirmed specific staining of ASC and NLRP3 through analysis of supernatants of *Pycard*$^{-/-}$ or *Nlrp3*$^{-/-}$ macrophages (**Fig. 2g**). The NLRP3 released from *Pycard*$^{-/-}$ macrophages after stimulation of the inflammasome formed extracellular particles (**Fig. 2g**). However, caspase-1 deficiency impaired the release of oligomeric particles of both ASC and NLRP3 (**Fig. 2g**). These data suggested that the little release of NLRP3 from caspase-1-deficient macrophages detected by immunoblot analysis (**Fig. 1f**) might have represented a small fraction of soluble NLRP3 that was unable to form detectable specks, which would indicate abundant release of oligomeric particles of inflammasomes via caspase-1-dependent pyroptosis. Macrophages stimulated by various inducers of NLRP3, as well as inducers of NLRP1, NLRC4 and AIM2, released significant amounts of ASC specks ($P < 0.05$; **Supplementary Fig. 2d**). In confirmation of the results obtained by crosslinking experiments, we found extracellular inflammasome particles at early time points after stimulation of NLRP3 (**Supplementary Fig. 2e**), and 54.06% ± 7.82% of extracellular ASC$^+$ particles detected by flow cytometry were also NLRP3$^+$ (mean ± s.e.m. of $n = 11$ independent experiments; data not shown). These data suggested that activation of caspase-1 controlled the release of oligomeric inflammasome particles composed of NLRP3 and ASC and did so probably by inducing pyroptosis.

Extracellular ASC specks activate caspase-1

We characterized caspase-1 activity in macrophage supernatants upon activation of the inflammasome, since detection of the mature subunits of caspase-1 by immunoblot analysis would not necessarily indicate that this extracellular caspase-1 is active, because potential association with inhibitors or inappropriate folding in a cell-free environment could result in an inactive enzyme. Using cleavage of the caspase-1-specific fluorescent substrate z-YVAD-AFC as a measure of caspase-1 activity, we found that supernatants of wild-type macrophages in which NLRP3 had been stimulated with ATP and nigericin had between 5 and 8 enzyme activity units of active caspase-1 (**Fig. 3a**). Extracellular caspase-1 activity after stimulation of the NLRP3 inflammasome was absent from *Nlrp3*$^{-/-}$ or *Pycard*$^{-/-}$ macrophages (**Fig. 3a**). Extracellular caspase-1 released from macrophages treated with ATP or nigericin was able to process pro-IL-1β in a cell-free environment in a manner similar to that used by recombinant caspase-1 (**Fig. 3b**). We also found significant correlation for the activation of caspase-1 over time in supernatants incubated without cells after stimulation of NLRP3 (**Fig. 3c**), which indicated that extracellular inflammasome oligomers were able to process pro-caspase-1 in supernatants. Such activation was absent from supernatants of *Nlrp3*$^{-/-}$ macrophages that did not release ASC or pro-caspase-1 upon stimulation (**Fig. 3c**).

To study the function of extracellular particles of ASC, we produced and purified recombinant oligomeric ASC specks tagged with yellow fluorescent protein (ASC-YFP) from HEK293 human embryonic kidney cells, a procedure made possible by the fact that transfection of cells to express ASC-YFP leads to spontaneous aggregation of ASC into a single speck (**Supplementary Fig. 3a**). Recombinant ASC-YFP$^+$ particles appeared as fiber-like structures by fluorescence microscopy (**Fig. 3d**) and were gated in the same region as that of ASC specks released from macrophages, when analyzed by flow cytometry on the basis of forward scatter versus side scatter (**Supplementary Fig. 3b**). Published reports

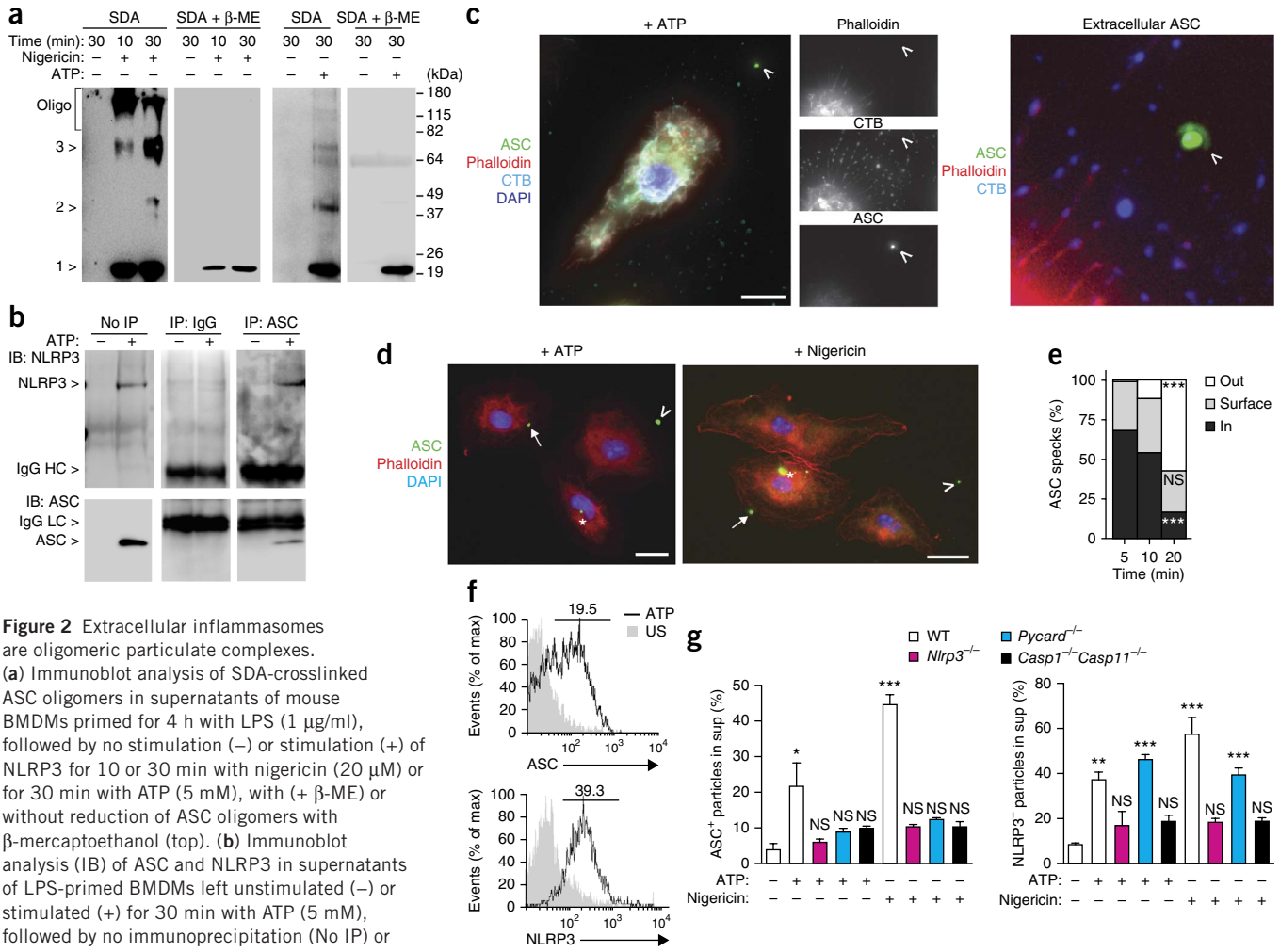

Figure 2 Extracellular inflammasomes are oligomeric particulate complexes. (**a**) Immunoblot analysis of SDA-crosslinked ASC oligomers in supernatants of mouse BMDMs primed for 4 h with LPS (1 μg/ml), followed by no stimulation (–) or stimulation (+) of NLRP3 for 10 or 30 min with nigericin (20 μM) or for 30 min with ATP (5 mM), with (+ β-ME) or without reduction of ASC oligomers with β-mercaptoethanol (top). (**b**) Immunoblot analysis (IB) of ASC and NLRP3 in supernatants of LPS-primed BMDMs left unstimulated (–) or stimulated (+) for 30 min with ATP (5 mM), followed by no immunoprecipitation (No IP) or immunoprecipitation with immunoglobulin G (IP: IgG) or antibody to ASC (IP: ASC). HC, heavy chain; LC, light chain. (**c**,**d**) Microscopy of BMDMs primed as in **a**, then stimulated for 30 min as in **a** with ATP (**c**,**d**) or with nigericin (**d**), followed by staining of ASC (green), actin (red; phalloidin), membranes (cyan; cholera toxin B (CTB) (**c**)) and nuclei (blue; DNA-binding dye DAPI); arrowheads, particulate ASC specks outside the cell; arrows, ASC specks near the cell edge; *, intracellular ASC specks. Right (**c**), 5× enlargement of image at far left. Scale bars, 10 μm. (**e**) Quantification of intracellular ASC specks (In), ASC specks near the macrophage edge (Surface) and extracellular ASC specks (Out) after stimulation of NLRP3 for 5, 10 or 20 min (horizontal axis) with ATP as in **a**, among total ASC specks. (**f**) Flow cytometry of supernatants of wild-type macrophages primed for 4 h with LPS (1 μg/ml), followed by no stimulation (US) or stimulation for 30 min with ATP (5 mM). Numbers above lines in plots indicate percent extracellular ASC$^+$ particles (top) or NLRP3$^+$ particles (bottom). (**g**) Frequency of extracellular ASC$^+$ particles (left) or NLRP3$^+$ particles (right) in cell-free supernatants of wild-type, *Nlrp3*$^{-/-}$, *Pycard*$^{-/-}$ or *Casp1*$^{-/-}$*Casp11*$^{-/-}$ macrophages primed as in **f**, followed by no stimulation (–) or stimulation (+) for 30 min with nigericin (20 μM) or with ATP (5 mM), presented relative to the total particles gated for small particles. *$P < 0.01$, **$P < 0.005$ and ***$P < 0.001$, for results at 20 min versus those at 5 or 10 min (**e**) or compared with unstimulated cells (**g**) (analysis of variance (ANOVA) with Bonferroni's post-test). Data are representative of at least three independent experiments (**a**–**d**,**f**), two (20 min), three (5 min) or four (for 10 min) independent experiments with >140 cells and >10 fields of view for each time point and experiment (**e**; mean), or three (nigericin) or five (ATP) independent experiments (**g**; mean and s.e.m.).

have demonstrated that ASC polymerizes into a prion-like speck[8,9], and examination of recombinant ASC-YFP by electron microscopy revealed large aggregates of fibers (**Fig. 3e**). That structure was similar to the speck identified by electron microscopy in macrophages treated with nigericin (**Fig. 3f** and **Supplementary Fig. 3c**) and had a fiber-like composition and was approximately 2 μm in diameter (data not shown). That size was similar to the size we noted for extracellular inflammasomes detected by flow cytometry (**Supplementary Fig. 2c**) and the reported size of inflammasome structures[9]. Electron microscopy of macrophages containing inflammasome specks also revealed separation of the cytoplasm, with approximately half of it well structured (with visible organelles and intact plasma membrane) and the rest of the cytoplasm completely composed of vacuoles and without structure, with numerous autophagy vesicles. The inflammasome oligomeric speck was present between the structured and unstructured parts of the cytoplasm or, in some cells, in the unstructured part of the cytoplasm near the cell edge, where the integrity of the plasma membrane was compromised (**Fig. 3f** and **Supplementary Fig. 3c**). To further confirm the functionality of recombinant ASC-YFP specks, we found that they were able to nucleate soluble ASC-mCherry to form larger mixed aggregates of ASC (**Fig. 3g**).

The addition of recombinant ASC-YFP$^+$ oligomeric specks to cell-free supernatants of macrophages that had been previously activated with various concentrations of nigericin resulted in an increase of caspase-1 activity in supernatants of wild-type macrophages but not in those of *Nlrp3*$^{-/-}$ macrophages (**Fig. 3h**). The potentiation of caspase-1 activity by ASC-YFP oligomers in cell-free supernatants was abolished when we used a buffer with 150 mM KCl or when ATP was

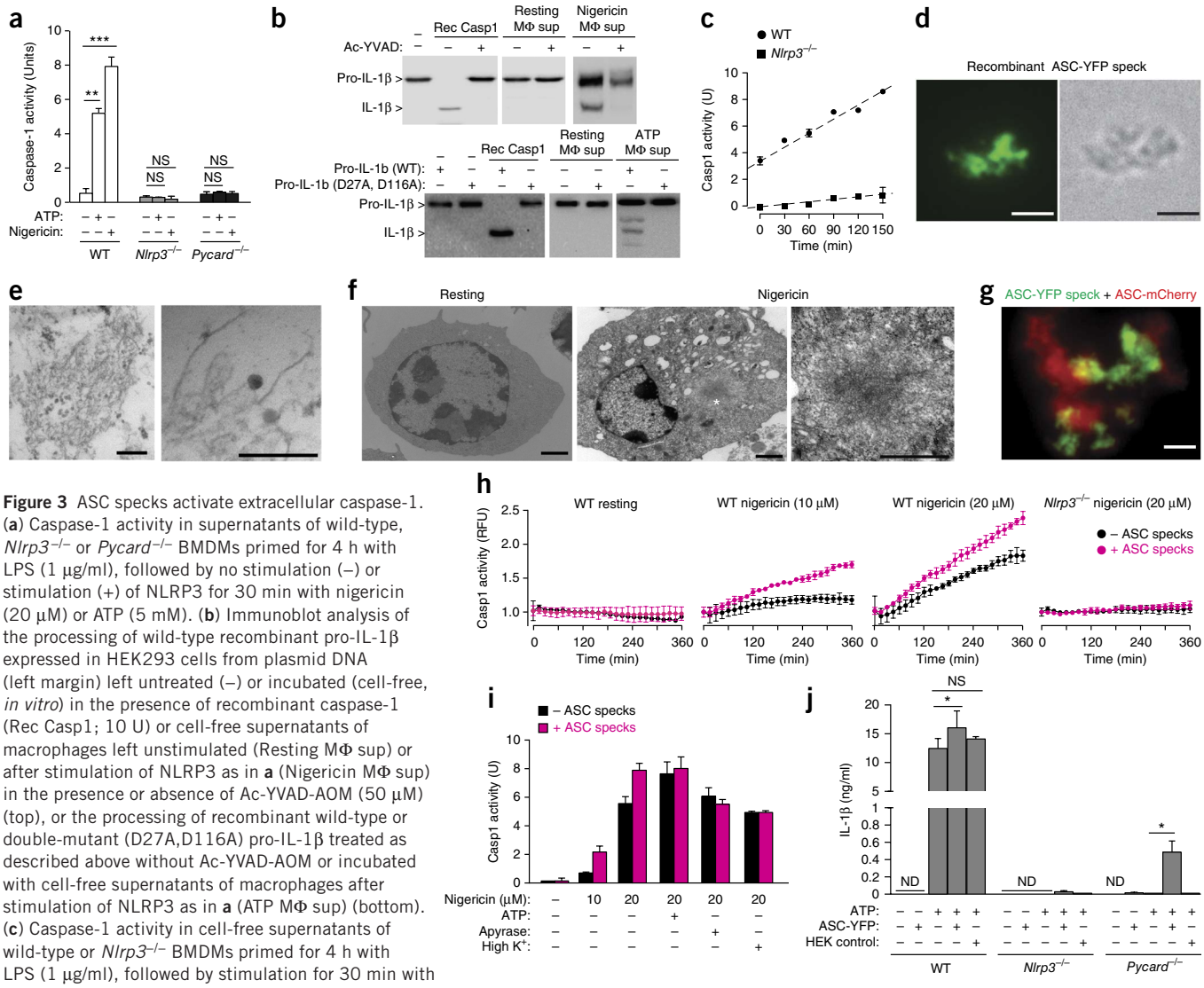

Figure 3 ASC specks activate extracellular caspase-1. (**a**) Caspase-1 activity in supernatants of wild-type, *Nlrp3*$^{-/-}$ or *Pycard*$^{-/-}$ BMDMs primed for 4 h with LPS (1 μg/ml), followed by no stimulation (–) or stimulation (+) of NLRP3 for 30 min with nigericin (20 μM) or ATP (5 mM). (**b**) Immunoblot analysis of the processing of wild-type recombinant pro-IL-1β expressed in HEK293 cells from plasmid DNA (left margin) left untreated (–) or incubated (cell-free, *in vitro*) in the presence of recombinant caspase-1 (Rec Casp1; 10 U) or cell-free supernatants of macrophages left unstimulated (Resting MΦ sup) or after stimulation of NLRP3 as in **a** (Nigericin MΦ sup) in the presence or absence of Ac-YVAD-AOM (50 μM) (top), or the processing of recombinant wild-type or double-mutant (D27A,D116A) pro-IL-1β treated as described above without Ac-YVAD-AOM or incubated with cell-free supernatants of macrophages after stimulation of NLRP3 as in **a** (ATP MΦ sup) (bottom). (**c**) Caspase-1 activity in cell-free supernatants of wild-type or *Nlrp3*$^{-/-}$ BMDMs primed for 4 h with LPS (1 μg/ml), followed by stimulation for 30 min with nigericin (10 μM) and then incubated for 0–150 min at 37 °C without cells. $r = 0.9848$; $P = 0.0003$ (Pearson's test). (**d**) Fluorescence microscopy (left) and brightfield microscopy (right) of recombinant ASC-YFP specks. Scale bars, 0.5 μm. (**e**) Transmission electron microscopy of recombinant ASC-YFP oligomeric specks (right, enlargement of the complex). Scale bars, 200 nm. (**f**) Transmission electron microscopy of wild-type macrophages left unstimulated (Resting) or stimulated for 30 min with nigericin (20 μM, Nigericin); right, enlargement of the fiber-like structure (*) at left. Scale bars, 1 μm. (**g**) Fluorescence microscopy of recombinant ASC-YFP specks nucleating soluble ASC-mCherry *in vitro*. Scale bar, 1 μm. (**h**,**i**) Caspase-1 activity in cell-free supernatants of wild-type BMDMs (**h**,**i**) or *Nlrp3*$^{-/-}$ BMDMs (**h**) activated for 30 min with various doses of nigericin (above (**h**) or below (**i**) plots), followed by incubation of cell-free supernatants for 0–360 min alone (–ASC specks) or with 5×10^5 recombinant ASC-YFP particles (+ASC specks) without additional reagents (**h**) or in the presence (+) or absence (–) of ATP (5 mM), apyrase (3 U/ml) or 150 mM KCl (High K^+) (**i**). RFU, relative fluorescent units. (**j**) Enzyme-linked immunosorbent assay (ELISA) of IL-1β released from LPS-primed, immortalized wild-type, *Nlrp3*$^{-/-}$ or *Pycard*$^{-/-}$ mouse BMDMs after stimulation of NLRP3 for 30 min with ATP (5 mM) and recombinant ASC-YFP specks (1:1, specks/cells) or HEK293 cell lysates (HEK control). ND, not detected. $^*P < 0.05$, $^{**}P < 0.005$ and $^{***}P < 0.001$ (Student's *t*-test). Data are from three (**a**), two (**c**) or four (**h**,**i**) independent experiments (mean and s.e.m.) or nine (wild type) or six (*Nlrp3*$^{-/-}$ and *Pycard*$^{-/-}$) independent experiments (**j**; mean and s.e.m.) or are representative of three (**b**,**e**–**g**) or four (**d**) independent experiments.

degraded by apyrase (**Fig. 3i**). The addition of recombinant ASC-YFP$^+$ oligomeric specks to macrophages together with ATP enhanced the release of IL-1β from wild-type or *Pycard*$^{-/-}$ macrophages but not from *Nlrp3*$^{-/-}$ macrophages (**Fig. 3j** and **Supplementary Fig. 3d**). These data suggested that extracellular oligomeric particles of ASC were able to rectify the deficiency in intracellular ASC in *Pycard*$^{-/-}$ macrophages during stimulation with ATP. As a control, we subjected lysates of mock-transfected HEK293 cells to the same purification protocol as that used for the ASC specks and found that the resulting products did not induce the release of IL-1β from macrophages (**Fig. 3j**). Extracellular recombinant ASC-YFP$^+$ specks were also able to restore the activation of caspase-1 in *Pycard*$^{-/-}$ macrophages, but not in *Nlrp3*$^{-/-}$ macrophages, after stimulation with ATP (**Supplementary Fig. 3f**). The potentiation effect of extracellular ASC-YFP$^+$ oligomeric particles was more evident when we incubated them for 3 h together with suboptimal concentrations of ATP or monosodium urate crystals (**Supplementary Fig. 3f**). In these experiments, in which we stimulated cells for 3 or 16 h, we found that recombinant ASC-YFP$^+$ specks alone induced the release of IL-1β (**Supplementary Fig. 3f**) and that the macrophages ingested ASC-YFP$^+$ particles (**Fig. 4a**).

By increasing the number of recombinant ASC-YFP$^+$ particles per macrophage, we were able to increase the release of IL-1β over 3 h

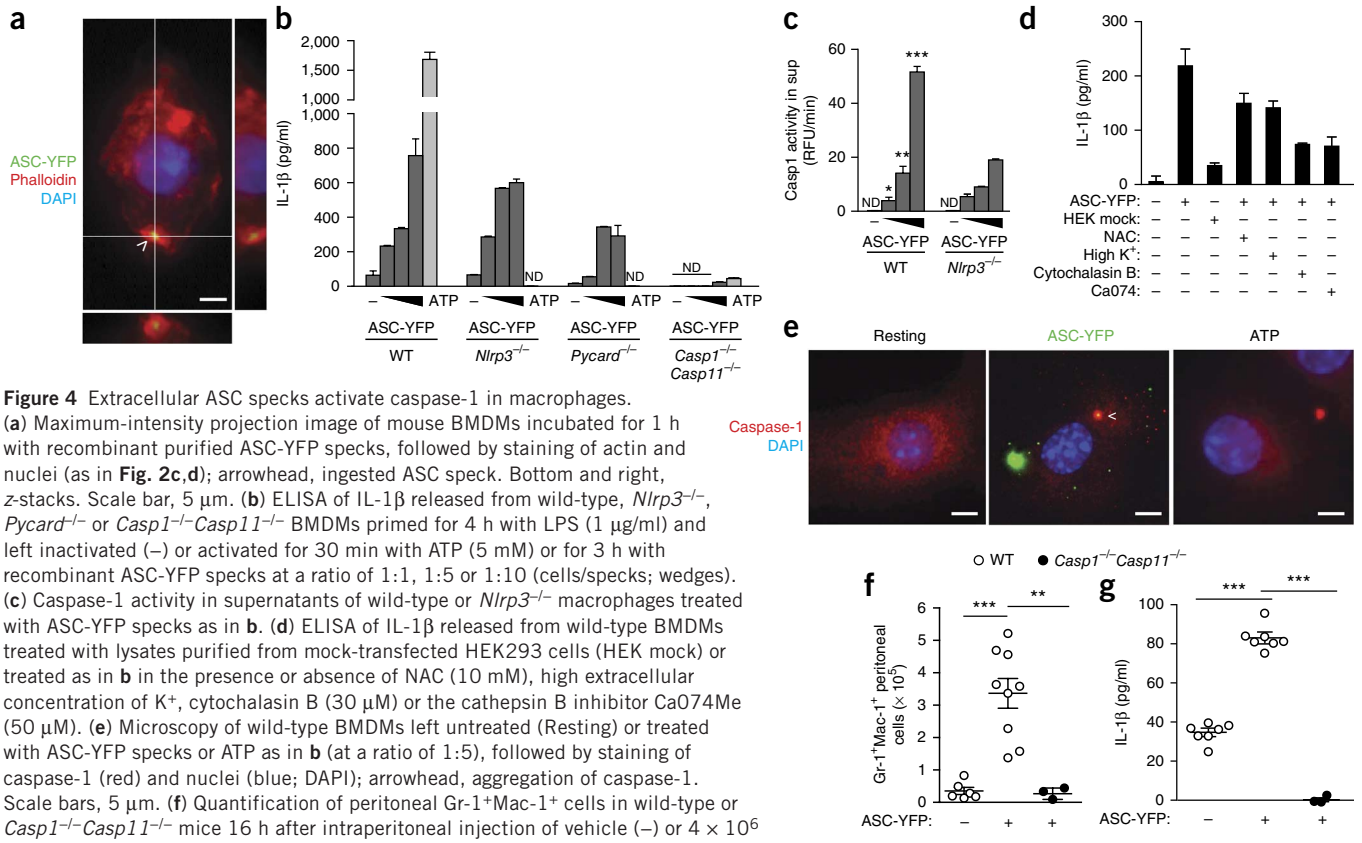

Figure 4 Extracellular ASC specks activate caspase-1 in macrophages. (**a**) Maximum-intensity projection image of mouse BMDMs incubated for 1 h with recombinant purified ASC-YFP specks, followed by staining of actin and nuclei (as in **Fig. 2c**,**d**); arrowhead, ingested ASC speck. Bottom and right, *z*-stacks. Scale bar, 5 μm. (**b**) ELISA of IL-1β released from wild-type, *Nlrp3*$^{-/-}$, *Pycard*$^{-/-}$ or *Casp1*$^{-/-}$*Casp11*$^{-/-}$ BMDMs primed for 4 h with LPS (1 μg/ml) and left inactivated (–) or activated for 30 min with ATP (5 mM) or for 3 h with recombinant ASC-YFP specks at a ratio of 1:1, 1:5 or 1:10 (cells/specks; wedges). (**c**) Caspase-1 activity in supernatants of wild-type or *Nlrp3*$^{-/-}$ macrophages treated with ASC-YFP specks as in **b**. (**d**) ELISA of IL-1β released from wild-type BMDMs treated with lysates purified from mock-transfected HEK293 cells (HEK mock) or treated as in **b** in the presence or absence of NAC (10 mM), high extracellular concentration of K^+, cytochalasin B (30 μM) or the cathepsin B inhibitor Ca074Me (50 μM). (**e**) Microscopy of wild-type BMDMs left untreated (Resting) or treated with ASC-YFP specks or ATP as in **b** (at a ratio of 1:5), followed by staining of caspase-1 (red) and nuclei (blue; DAPI); arrowhead, aggregation of caspase-1. Scale bars, 5 μm. (**f**) Quantification of peritoneal Gr-1$^+$Mac-1$^+$ cells in wild-type or *Casp1*$^{-/-}$*Casp11*$^{-/-}$ mice 16 h after intraperitoneal injection of vehicle (–) or 4 × 10^6 purified recombinant ASC-YFP specks (+). (**g**) ELISA of IL-1β in peritoneal lavage fluid from wild-type or *Casp1*$^{-/-}$*Casp11*$^{-/-}$ mice treated as in **f**. Each symbol (**f**,**g**) represents an individual mouse; small horizontal lines indicate the mean (± s.e.m.). $*P < 0.05$, $**P < 0.005$ and $***P < 0.001$ (Student's *t*-test). Data represent three independent experiments (mean and s.e.m. in **b**–**d**).

of incubation (**Fig. 4b**). In these conditions, the release of IL-1β was independent of ASC and NLRP3 but was completely dependent on caspase-1 (**Fig. 4b**). The addition of recombinant ASC-YFP$^+$ specks also increased caspase-1 activity in wild-type macrophages and, to a lesser extent, in *Nlrp3*$^{-/-}$ macrophages (**Fig. 4c**). The release of IL-1β induced by incubation with ASC-YFP was substantially inhibited when we blocked phagocytosis through the use of cytochalasin B or when we applied the cathepsin B inhibitor Ca074, but not when we used a high extracellular concentration of K^+ or the antioxidant NAC (N-acetyl-L-cysteine) (**Fig. 4d**). As a control, purified preparations of mock-transfected HEK293 cells did not induce the release of IL-1β from macrophages (**Fig. 4d**). Upon internalizing particles of ASC-YFP, macrophages with ingested ASC-YFP$^+$ specks presented aggregates of caspase-1, similar to those found in macrophages activated by ATP (**Fig. 4e**). Intraperitoneal injection of oligomeric particles of ASC-YFP into mice resulted in an increase in the number of peritoneal granulocytes recruited in wild-type mice but not in *Casp1*$^{-/-}$*Casp11*$^{-/-}$ mice (**Fig. 4f**), and this also increased the amount of IL-1β in the peritoneum of wild-type mice (**Fig. 4g**). Our data support the proposal of a dual role for extracellular ASC specks in modulating caspase-1 activity. These can directly regulate caspase-1 in the extracellular environment, as well as after being internalized by macrophages, by directly nucleating and activating pro-caspase-1. In the latter case, NLRP3 is not required when oligomeric ASC is internalized by macrophages.

Extracellular mutant NLRP3 specks activate caspase-1

To study the possible function of extracellular active particles of NLRP3, we generated constitutively activated NLRP3 mutants associated with CAPS and expressed them in HEK293 cells. The expression of various recombinant CAPS-associated NLRP3 mutants (with the substitutions p.R260W, p.T348M and p.D303N, where 'p.' indicates the substitution is in the protein) in HEK293 cells resulted in the spontaneous self-oligomerization of mutant NLRP3 into specks, but expression of recombinant wild-type NLRP3 did not (**Fig. 5a**). For HEK293 cells expressing both the purinergic receptor P2X7 and a recombinant YFP-tagged version of the NLRP3 mutant p.D303N (NLRP3(p.D303N)-YFP), extracellular stimulation with ATP resulted in the release of oligomeric particles of NLRP3(p.D303N)-YFP into the cell supernatant, as was evident by fluorescence microscopy (**Fig. 5b**), flow cytometry (**Fig. 5c**) and immunoblot analysis (**Fig. 5d**). For HEK293 cells expressing P2X7, treatment with ATP resulted in permeabilization of the plasma membrane to YOPRO-1 and a significant increase in cell death, as assessed by release of LDH (**Fig. 5e**). We next purified recombinant NLRP3(p.D303N)-YFP particles from HEK293 cells (**Fig. 5f**) and analyzed their ultrastructure by electron microscopy. Different from recombinant ASC-YFP specks, oligomeric particles of NLRP3(p.D303N)-YFP appeared to be smaller in size and were compact globular aggregates (**Fig. 5g**) that were able to aggregate red fluorescent protein–tagged ASC when these were expressed together in HEK293 cells (**Fig. 5h**), similar to what has been proposed for the active NLRP3 heads that serve as scaffolding for the oligomerization of ASC fibers into a large particle[8,9].

To determine if oligomeric particles of NLRP3(p.D303N)-YFP were functional extracellularly, we incubated them with cell-free supernatants of ATP-treated macrophages. We found that particles of NLRP3(p.D303N)-YFP localized together with ASC released from macrophages (**Fig. 5i**), which suggested that they were able to nucleate extracellular ASC in a cell-free environment. We further confirmed

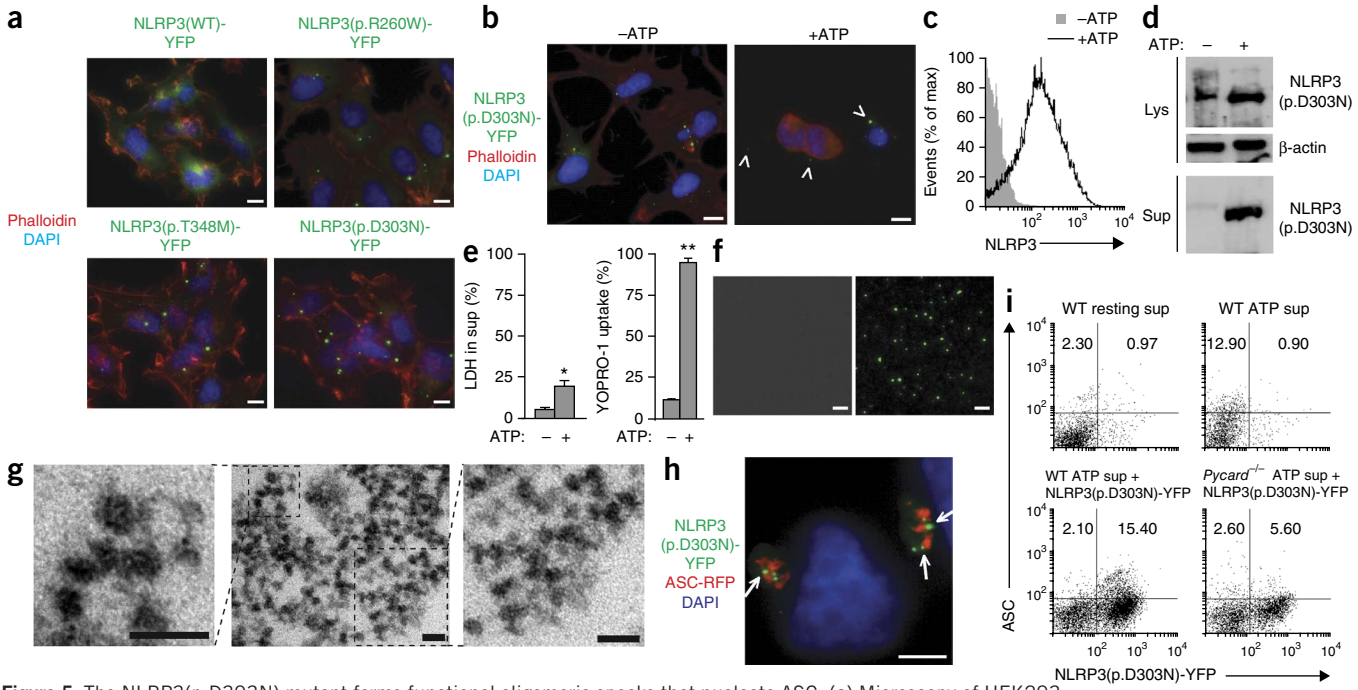

Figure 5 The NLRP3(p.D303N) mutant forms functional oligomeric specks that nucleate ASC. (**a**) Microscopy of HEK293 cells expressing YFP-tagged wild-type NLRP3 (NLRP3(WT)-YFP) or CAPS-associated NLRP3 mutants (NLRP3(p.R260W)-YFP, NLRP3(p.T348M)-YFP and NLRP3(p.D303N)-YFP), with staining of actin and nuclei (as in **Fig. 2c**). Scale bars, 10 μm. (**b**) Microscopy of HEK293 cells expressing the receptor P2X7 and the NLRP3(p.D303N)-YFP mutant, left untreated (–ATP) or treated for 30 min with ATP (3 mM) (+ATP) and stained as in **a**; arrowheads, NLRP3(p.D303N)-YFP particles released from cells. Scale bars, 10 μm. (**c**,**d**) Flow cytometry (**c**) and immunoblot analysis (**d**) of supernatants (**c**,**d**) and lysates (**d**) of cells treated as in **b**, detecting extracellular NLRP3(p.D303N)-YFP particles. (**e**) Abundance of LDH in supernatants of cells treated as in **b** (left) and frequency of such cells permeable to YOPRO-1 (right), among total intracellular LDH (left) or total cells (right). $^{*}P < 0.005$ and $^{**}P < 0.001$ (Student's *t*-test). (**f**) Fluorescence microscopy (right) and brightfield microscopy (left) of purified recombinant NLRP3(p.D303N)-YFP particles. Scale bars, 5 μm. (**g**) Transmission electron microscopy of purified recombinant NLRP3(p.D303N)-YFP particles. Scale bars, 50 nm. (**h**) Microscopy of HEK293 cells expressing the NLRP3(p.D303N)-YFP mutant and red fluorescent protein–tagged ASC (ASC-RFP), with DAPI staining of nuclei (blue); arrows, NLRP3(p.D303N)-YFP serving as an oligomerization 'head' for ASC-RFP. Scale bar, 5 μm. (**i**) Flow cytometry of cell-free supernatants of wild-type or *Pycard*$^{-/-}$ mouse BMDMs primed for 4 h with LPS (1 μg/ml) left untreated (resting) or treated for 30 min with ATP (5 mM) (ATP), followed by incubation of cell-free supernatants in the presence (bottom row) or absence (top row) of 5×10^5 NLRP3(p.D303N)-YFP particles and staining of ASC. Numbers in plots indicate percent ASC^{+}NLRP3^{-} particles (left) or ASC^{+}NLRP3^{+} particles (right). (**j**) Microscopy of recombinant NLRP3(p.D303N)-YFP particles nucleating soluble ASC-mCherry (arrows). Scale bars, 2 μm. Data are representative of three (**a**,**b**,**f**–**h**,**j**), two (**c**,**d**,**i**) or four (**e**) independent experiments (mean and s.e.m. in **e**).

this by fluorescence microscopy in which oligomeric particles of NLRP3(p.D303N)-YFP served as scaffolds for the oligomerization of soluble ASC (**Fig. 5j**).

By immunofluorescence and immunoblot analysis of cell lysates, we found that macrophages were able to ingest recombinant NLRP3(p.D303N)-YFP particles by phagocytosis (**Supplementary Fig. 4a**,**b**) without inducing substantial cell death (**Supplementary Fig. 4c**). The addition of oligomeric particles of recombinant NLRP3(p.D303N)-YFP to wild-type or *Nlrp3*$^{-/-}$ macrophages increased the release of IL-1β (**Fig. 6a**,**b**), activated caspase-1 (**Fig. 6c**) and induced the formation of endogenous ASC specks (**Fig. 6d**,**e**), with the subsequent release of oligomeric particles of ASC, as detected by flow cytometry (**Fig. 6f**). However, NLRP3(p.D303N)-YFP particles did not induce the release of IL-1β from or activation of caspase-1 in *Pycard*$^{-/-}$ macrophages (**Fig. 6b**,**c**). These data suggested that extracellular particles in the form of the gain-of-function NLRP3(p.D303N) mutant needed ASC to activate caspase-1, as ASC is the adaptor that links NLRP3 oligomers to pro-caspase-1.

We observed phagocytosis of NLRP3(p.D303N)-YFP particles in 33% of macrophages containing ASC specks (**Supplementary Fig. 4d**). Blockade of the internalization of NLRP3(p.D303N)-YFP particles with cytochalasin B reduced the release of IL-1β by 69% (**Fig. 6g**) and decreased the number of macrophages with ASC specks by 31% (**Supplementary Fig. 4e**). Recombinant NLRP3(p.D303N)-YFP particles were able to induce the release of IL-1β from macrophages when we used a buffer with a high extracellular concentration of K^+ and when we used the antioxidant NAC or the cathepsin B inhibitor Ca074 (**Fig. 6h**). These data showed that the efflux of K^+ from the cell, generation of reactive oxygen species and cathepsin B activity required for the formation of new NLRP3 aggregates were not necessary when macrophages internalized preassembled particles of active NLRP3. Intraperitoneal injection of specks of recombinant NLRP3(p.D303N)-YFP into wild-type mice resulted in a substantial increase in the number of peritoneal granulocytes (**Fig. 6i**), as well as increased production of IL-1β (**Fig. 6j**), that was absent from *Pycard*$^{-/-}$ mice (**Fig. 6i**,**j**). Therefore, constitutively active NLRP3 proteins were able to 'self-oligomerize' in the absence of ASC into particles that were released from cells, and after being internalized by surrounding macrophages, they were able to activate caspase-1 by recruiting ASC.

Inflammasome particles in the serum of patients with CAPS

CAPS are the consequence of rare, heterozygous, gain-of-function mutations in *NLRP3* and include three clinical phenotypes of increasing

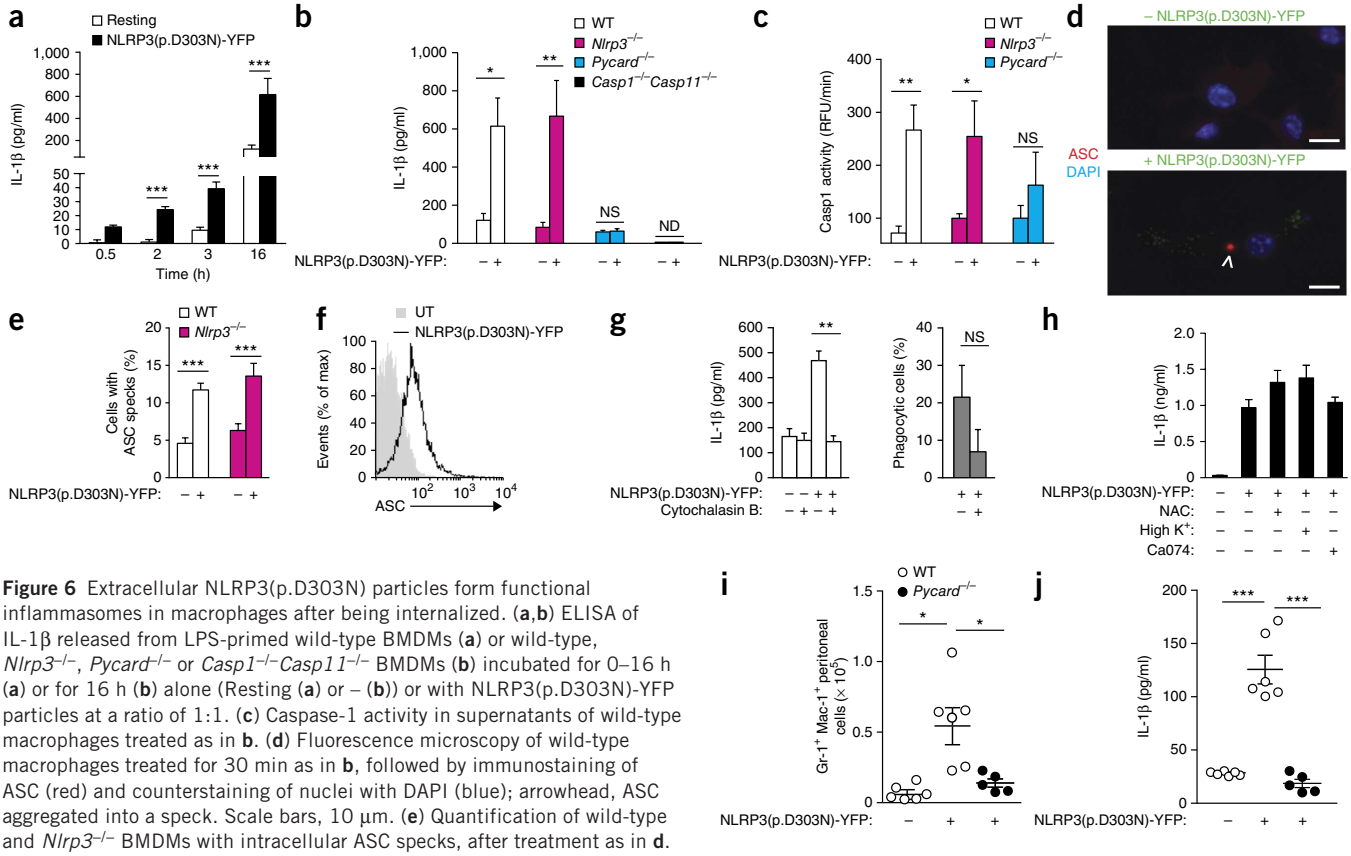

Figure 6 Extracellular NLRP3(p.D303N) particles form functional inflammasomes in macrophages after being internalized. (**a**,**b**) ELISA of IL-1β released from LPS-primed wild-type BMDMs (**a**) or wild-type, *Nlrp3*$^{-/-}$, *Pycard*$^{-/-}$ or *Casp1*$^{-/-}$*Casp11*$^{-/-}$ BMDMs (**b**) incubated for 0–16 h (**a**) or for 16 h (**b**) alone (Resting (**a**) or – (**b**)) or with NLRP3(p.D303N)-YFP particles at a ratio of 1:1. (**c**) Caspase-1 activity in supernatants of wild-type macrophages treated as in **b**. (**d**) Fluorescence microscopy of wild-type macrophages treated for 30 min as in **b**, followed by immunostaining of ASC (red) and counterstaining of nuclei with DAPI (blue); arrowhead, ASC aggregated into a speck. Scale bars, 10 μm. (**e**) Quantification of wild-type and *Nlrp3*$^{-/-}$ BMDMs with intracellular ASC specks, after treatment as in **d**. (**f**) ASC particles in supernatants of wild-type macrophages left untreated (UT) or treated for 3 h as in **b**, detected by flow cytometry. (**g**,**h**) ELISA of IL-1β released from LPS-primed wild-type mouse BMDMs left unstimulated (–) or stimulated (+) for 16 h with NLRP3(p.D303N)-YFP particles and left untreated (–) or treated (+) with cytochalasin B (20 μM) (**g**) or with NAC (10 mM), a high extracellular concentration of K^+ or Ca074Me (50 μM) (**h**). Right (**g**), phagocytosis of NLRP3(p.D303N)-YFP particles by BMDMs as at left, stimulated for 16 h with NLRP3(p.D303N)-YFP particles and left untreated or treated with cytochalasin B. (**i**) Peritoneal Gr-1$^+$Mac-1$^+$ cells in wild-type and *Pycard*$^{-/-}$ mice 16 h after intraperitoneal injection of vehicle (–) or 4×10^6 purified recombinant NLRP3(p.D303N)-YFP particles (+). (**j**) ELISA of IL-1β in peritoneal lavage fluid from mice treated as in **i**. Each symbol (**i**,**j**) represents an individual mouse; small horizontal lines indicate the mean (± s.e.m.). $^*P < 0.05$, $^{**}P < 0.005$ and $^{***}P < 0.001$ (Student's *t*-test). Data are representative of three (0.5 h and 2 h) or ten (3 h and 16 h) independent experiments (**a**; mean and s.e.m.) or eight (**b**), four (**c**), two (**d**,**f**) or three (**g**–**j**) independent experiments (mean and s.e.m. in **b**,**c**,**g**,**h**) or two independent experiments with >300 cells and four to eight fields of view in each (**e**; mean and s.e.m.).

severity. These range from the least severe phenotype, familial cold autoinflammatory syndrome, to Muckle-Wells syndrome, to the most severe phenotype, chronic infantile neurological, cutaneous and articular syndrome[28]. The data reported above showed that NLRP3 gain-of-function mutants correlated with the aggregation of NLRP3 into particles with proinflammatory extracellular activity that induced the release of ASC specks. We therefore assessed the presence of particles of ASC and NLRP3 in the serum of patients with CAPS during symptom-free intervals and during acute inflammatory episodes. By fluorescence microscopy and flow cytometry, we discovered ASC$^+$ particles in the serum of patients with each clinical phenotype of CAPS (**Fig. 7a**,**b** and **Supplementary Table 1**). We then confirmed that the protocol of isolating serum by centrifugation did not induce loss of inflammasome particles (**Supplementary Fig. 5a**) and that recombinant ASC-YFP$^+$ particles were gated in the same area as that of inflammasome particles from patients with CAPS, on the basis of forward scatter versus side scatter, which were adjusted to display correct separation of leukocyte populations (**Supplementary Fig. 5b**).

The serum of patients with active CAPS had pathological concentrations of C-reactive protein (CRP) of over 10 mg/l (**Fig. 7c**) and a significantly greater abundance of extracellular oligomeric ASC$^+$ particles than that in serum from healthy donors (**Fig. 7d**). However, there were no significant differences between the serum of healthy donors and that of patients with CAPS during symptom-free intervals (CRP < 10 mg/l) in terms of the abundance of ASC$^+$ particles (**Fig. 7d**). Staining indicating the abundance of ASC$^+$ particles in the serum of healthy donors was below the background staining of serum samples stained with secondary antibody alone (**Fig. 7d**). Among the various CAPS phenotypes, we detected a distinct tendency for high concentrations of CRP in the serum and a general tendency for elevated amounts of ASC$^+$ particles in the serum (**Supplementary Fig. 5c**,**e**). In eight of the fourteen patients with active CAPS whom we analyzed, the frequency of NLRP3$^+$ particles in the serum was above the average frequency of such particles in the serum of healthy donors, with a particularly greater abundance of NLRP3$^+$ particles in the serum of four of these patients (three with Muckle-Wells syndrome and one chronic infantile neurological, cutaneous and articular syndrome) (**Fig. 7e** and **Supplementary Table 1**). However, the greater abundance of NLRP3$^+$ particles in the serum of the patients with active CAPS relative to that of healthy donors seemed to have no statistical significance (**Fig. 7e**). This increase was also not significant when we stratified the patients with CAPS by clinical phenotype (**Supplementary Fig. 5d**). Among the seven patients with a greater abundance of ASC$^+$ and NLRP3$^+$ particles in serum, we found that 48.32% ± 7.82% of ASC$^+$ specks were

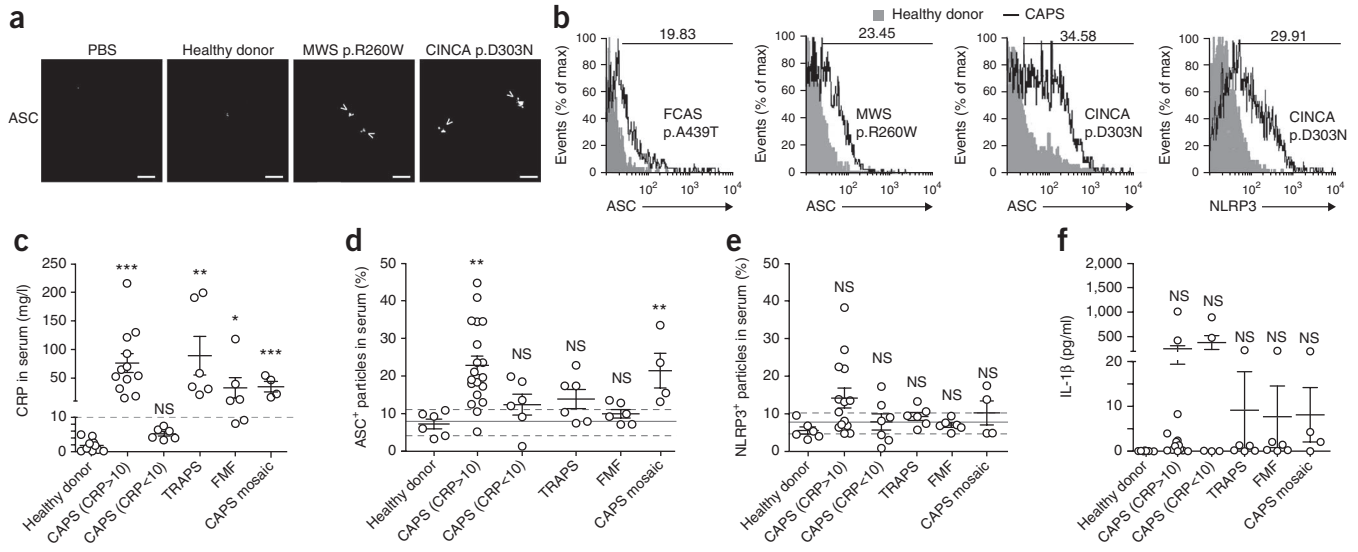

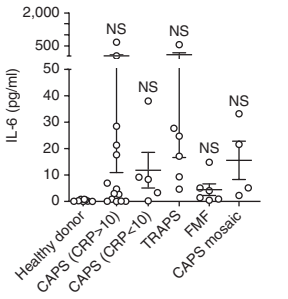

Figure 7 Extracellular inflammasome particles are present in the serum of patients with CAPS. (**a**) Fluorescence microscopy of sterile PBS (control) or serum from a healthy human donor or patients with active CAPS (Muckle-Wells syndrome (MWS) or chronic infantile neurological, cutaneous and articular syndrome (CINCA); mutant NLRP3 substitutions, above images), immunostained for ASC; arrowheads, ASC aggregates. Scale bars, 50 μm. (**b**) Flow cytometry of serum of patients with active CAPS (as in **a** and familial cold autoinflammatory syndrome (FCAS)) and healthy donors. Numbers above lines at top indicate percent ASC$^+$ particles (left and middle) or NLRP3$^+$ particles (far right). (**c**) CRP in the serum from healthy donors and patients with active CAPS (CRP > 10 mg/l) or during a symptom-free interval (CRP < 10 mg/l), patients with TNF receptor–associated periodic syndrome (TRAPS) or familial Mediterranean fever (FMF) and patients with CAPS with low-grade somatic *NLRP3* mosaicism (CAPS mosaic). (**d**,**e**) Frequency of ASC$^+$ particles (**d**) or NLRP3$^+$ particles (**e**) in serum from the groups in **c**, assessed by flow cytometry with gating for small particles and background staining established with the fluorescent secondary antibody alone presented as median (solid gray line) and 75th and 25th percentiles (dashed gray lines). (**f**) IL-1β and IL-6 in the serum of the groups in **c**. Each symbol (**c**–**f**) represents an individual patient; small horizontal lines indicate the mean (± s.e.m.). $^*P < 0.05$, $^{**}P < 0.005$ and $^{***}P < 0.001$, compared with healthy subjects (ANOVA with Dunnett's post-test). Data are representative of two experiments (**a**) or four (left), eight (middle left) or three (middle right and right) experiments (**b**) or are from one experiment with 46 subjects (**c**–**f**).

also NLRP3$^+$ (mean ± s.e.m.; data not shown), which demonstrated that the serum of patients with CAPS had ASC$^+$NLRP3$^+$ particles at an abundance similar to that found in supernatants of macrophages. We also evaluated the presence of ASC$^+$ and NLRP3$^+$ particles in the serum of patients with other inherited autoinflammatory syndromes unrelated to *NLRP3* mutations. In particular, we examined patients with familial Mediterranean fever who carry biallelic mutations of *MEFV* (which encodes pyrin), and patients with TNF receptor–associated periodic syndrome, who carry structural heterozygous mutations in *TNFRSF1A* (which encodes the TNF receptor CD120a). Although both groups of patients had higher serum concentrations of CRP than that of healthy donors (**Fig. 7c**), they did not have a significantly higher frequency of ASC$^+$ or NLRP3$^+$ particles in their serum than that of the group of healthy donors (**Fig. 7d**,**e**).

Among patients with CAPS, there is a rare group with low somatic *NLRP3* mosaicism that causes autoinflammatory phenotypes. We analyzed the serum of four patients with a range of somatic *NLRP3* mosaicism of 9–31% during active disease (**Supplementary Table 1**). We found that the patients with CAPS who had somatic mosaicism had significantly more oligomeric ASC$^+$ particles in the serum than did healthy donors (**Fig. 7d**), and two patients also had more NLRP3$^+$ particles in the serum (**Fig. 7e**).

Although IL-1β drives the clinical phenotype of CAPS, only some patients with CAPS had a higher concentration of IL-1β, independently of their phenotype or serum concentration of CRP, than that of healthy donors (**Fig. 7f**, **Supplementary Fig. 5g** and **Supplementary Table 1**). Serum concentrations of IL-1β were variable among patients with different types of CAPS, and we were unable to find any positive correlation with the serum concentration of CRP or with the presence of ASC$^+$ or NLRP3$^+$ particles in serum (**Supplementary Fig. 5f**). Some patients with active CAPS also had higher concentrations of the inflammatory cytokines IL-6 and TNF than did healthy donors (**Fig. 7f** and **Supplementary Table 1**), and these increased with the severity of CAPS (**Supplementary Fig. 5g**). Together these data suggested that ASC$^+$ particles might represent a biomarker for active CAPS and might be involved in the pathophysiology of the disease by activating surrounding macrophages.

DISCUSSION

In this study, we found that activation of inflammasomes led to the release of functional oligomeric inflammasome particles containing both NLRP3 and ASC that acted as danger signals to amplify inflammation by promoting the activation of caspase-1 extracellularly and in surrounding macrophages following internalization of the particles. Caspase-1 activity was necessary for the release of inflammasome particles from activated macrophages during pyroptosis. The released, extracellular caspase-1 was active and was able to mature pro-IL-1β. Both ASC and the structural, gain-of-function, CAPS-associated NLRP3 mutant p.D303N oligomerized into active particles of different composition that we detected in the serum of patients with active CAPS.

Caspase-1 is a protease that controls the release of various leaderless proteins, as well as its own release[24]. The 'caspase-1 secretome'

(all proteins released by a cell after activation of caspase-1) of macrophages includes the well-studied proinflammatory cytokines IL-1β and IL-18 and the alarmin HMGB1, as well as proteins that are not direct substrates of the protease, such as IL-1α or the fibroblast growth factor FGF-2 (refs. 23,24,29). The proteins released upon activation of caspase-1 are involved mainly in inflammation, cytoprotection and tissue repair[24]. The caspase-1-activating NLRP3 inflammasome controls the caspase-1 secretome, and here we additionally found that caspase-1 controlled the release of inflammasome oligomeric particles containing NLRP3 and ASC. This suggests an additional regulatory role for the inflammasome complex acting as an extracellular danger signal.

In macrophages, caspase-1 induces the specific type of cell death called 'pyroptosis', in which the cells quickly lose plasma membrane integrity and, at later stages, release intracellular proteins such as LDH[27]. This strategy is an efficient mechanism used to clear intracellular bacteria such as *Salmonella* or *Legionella*[30]. Here we found that caspase-1 controlled the release of inflammasome particles from macrophages at very early time points after the activation of inflammasomes (10–30 min after activation with ATP or nigericin), with an insignificant increase in extracellular LDH but with enhanced membrane permeabilization. Similarly, death induced in COS-7 monkey kidney cells by overexpression of ASC also leads to the presence of stable extracellular ASC specks[31]. LDH is a cytosolic protein with a molecular mass of 140 kDa and a diameter of 26.6 nm that is routinely used to monitor cell death; it is smaller than inflammasome particles (1–2 μm in diameter)[9], which suggests that pyroptosis might 'preferentially' result in the release of specific cytosolic components. This might be made possible through specific compartmentalization of the cytoplasm; electron microscopy of nigericin-treated macrophages revealed compartmentalization of the cytosol, with approximately half of the cytoplasm being well structured (with visible organelles and intact plasma membrane) and the rest of the cytoplasm made up of vacuoles and unstructured in phenotype, with numerous vesicles for autophagy. Autophagy has been proposed as a mechanism for limiting the activation of inflammasomes[32,33] but has also been proposed as a mechanism for the unconventional release of IL-1β upon caspase-1 activation[34]. The inflammasome speck was present between the structured and unstructured parts of the cytoplasm or near the edge of the cell in the unstructured part of the cytoplasm where plasma membrane integrity was compromised. These data suggest that the initial fast release of inflammasome particles could be the result of polarized cytoplasm in the macrophage during the early events of pyroptosis. Thus, while some of the protein pool (i.e., β-actin or LDH) might remain in the intracellular location in the 'normal' side of the cytoplasm, the inflammasome particle and probably also IL-1β are released through a 'focal' side of the cell. We found that a small pool of NLRP3 protein was also released a short time after the stimulation of inflammasomes (probably as a core component of particulate inflammasomes that were released). That was followed by delayed release of the rest of the soluble NLRP3; this fits with the kinetics of the release of LDH and β-actin, which suggests that most NLRP3 might leak from the cell after the inflammasome particle is released.

The immune system uses different extracellular strategies for the clearance of infectious agents and for the recovery of homeostasis; these include, for example, the formation of extracellular nets or circulating immunocomplexes[35,36]. It has been shown that extracellular neutrophil nets activate caspase-1 via the NLRP3 inflammasome in macrophages[37], and here we found that the multiprotein inflammasome complex acted as an extracellular danger particle to amplify the inflammatory response through the activation of caspase-1 in neighboring macrophages. The caspase-1 released after the activation of inflammasomes was active and was able to process pro-IL-1β in the extracellular milieu; this expands the known functions of caspase-1 to acting on extracellular substrates.

The NLRP3 inflammasome has been classically described as an oligomer consisting of the core sensor NLRP3, with ASC being the adaptor that recruits pro-caspase-1 (ref. 2). The activation of caspase-1 then involves autocleavage of pro-caspase-1 at residues Asp119, Asp297 and Asp316, which releases the large (p20) and small (p10) subunits from the amino-terminal caspase-recruitment domain[38]. In addition, upon activation of the NLRP3 inflammasome, most ASC in the cell oligomerizes into a large complex that was initially linked to pyroptosis and is called the 'pyroptosome'[39]. Ultrastructural studies have demonstrated that after being stimulated, NLRP3 proteins oligomerize and recruit ASC into fiber-like structures that form large particles[8,9]; this unifies the concepts of the NLRP3 inflammasome and the ASC speck. The oligomeric particles of recombinant ASC in our studies also appeared as fiber-like structures that were able to recruit new subunits of ASC and were able to activate caspase-1 in the extracellular environment. These particles were also internalized by macrophages and induced activation of caspase-1 and release of IL-1β independently of endogenous NLRP3 or ASC. In contrast to other protein aggregates that activate the NLRP3 inflammasome via lysosomal destabilization, such as β-amyloid or islet amyloid polypeptide[12,40], oligomers of ASC were able to induce the activation of caspase-1 by directly aggregating pro-caspase-1 in macrophages independently of NLRP3.

We also found extracellular inflammasome particles in the serum of patients with active CAPS. Oligomeric particles of NLRP3 with mutant gain-of-function subunits were internalized by macrophages and were able to induce ASC aggregation, caspase-1 activation and IL-1β release in NLRP3-deficient macrophages. It has been reported that germline and somatic *NLRP3* mutations cause CAPS with different clinical phenotypes[41,42]. How low somatic *NLRP3* mosaicism causes CAPS is poorly studied. Our data have provided new insight into the pathophysiological mechanisms that underlie CAPS and somatic *NLRP3* mosaicism, since released inflammasome oligomers containing mutant NLRP3 proteins were able to activate caspase-1 in monocytes and macrophages carrying exclusively wild-type *NLRP3* alleles. In fact, we found a greater abundance of ASC^+ particles in the serum of patients with CAPS who have low somatic *NLRP3* mosaicism. IL-1β is the main driver of the pathophysiology of CAPS, since various strategies used to block IL-1β (anakinra, canakinumab and rilonacept) quickly and completely resolve the clinical and biochemical features of this disease[43–45]. However, serum concentrations of IL-1β are not a good biomarker of disease for patients with CAPS, and the diagnosis of CAPS depends on *NLRP3* genotyping. It was unexpected that we found no significant difference between patients with CAPS during disease flares and healthy subjects in terms of the number of $NLRP3^+$ particles in the serum. The ratio of ASC to NLRP3 in inflammasome oligomeric particles is extremely high[9], and this could explain the greater difficulty in detecting NLRP3 in particles than in detecting ASC^+ particles in the serum of patients with CAPS. Furthermore, the antibody to NLRP3 we used here was raised against the amino-terminal pyrin-containing domain of NLRP3, the domain that interacts with ASC and is probably inaccessible to the antibody upon activation of the NLRP3 inflammasome by formation of the oligomeric NLRP3-ASC structure. That proposal is supported by studies showing that the efficacy with which NLRP3 is immunoprecipitated via a tag on the amino terminus of the protein decreases upon stimulation of NLRP3 (ref. 11); therefore, the amino-terminal epitope hidden in the inflammasome structure after oligomerization could also have affected the detection of NLRP3 in the ASC^+ particles

in the serum of patients with CAPS. Here we found that during active disease, patients with CAPS had enhanced serum concentrations of ASC^+ particles. We did not observe this in the serum of patients with the inherited autoinflammatory diseases familial Mediterranean fever or TNF receptor–associated periodic syndrome, which suggests that detection of ASC in serum could represent an additional strategy for the diagnosis and monitoring of CAPS. In support of this proposal, it has been reported that the detection of ASC in the cerebrospinal fluid of patients with brain injury correlates with their functional outcome[46]. Together our data have demonstrated that the activation of inflammasomes resulted in the release of active inflammasome oligomers as particles that acted extracellularly as danger signals to amplify the inflammatory response by activating caspase-1.

METHODS

Methods and any associated references are available in the online version of the paper.

Note: Any Supplementary Information and Source Data files are available in the online version of the paper.

ACKNOWLEDGMENTS

We thank E. Latz (Institute of Innate Immunity) for immortalized ASC-mCherry, ASC-deficient and NLRP3-deficient mouse bone marrow macrophages and for the expression vector encoding red fluorescent protein–tagged ASC; V. Dixit (Genentech) for *Pycard*$^{-/-}$ mice; M.C. Baños and J.J. Martínez for technical assistance with both molecular and cellular analyses; L. Martinez-Alarcón for extraction of blood from healthy donors; M. Martínez-Villanueva for analysis of CRP; and C. de Torre for support with proteomics. Supported by the Wellcome Trust (V.C.), Instituto Salud Carlos III (CD12/00523 and CD13/00059 to F.M.-S. and J.A.-I.), Instituto Salud Carlos III–Fondo Europeo de Desarrollo Regional (EMER07/049, PS09/00120 and PI13/00174 to P.P. and PS09/01182 to J.Y.), Fundación Séneca (11922/PI/09 to P.P.) and Fundación Mutua Madrileña (ID98FMM013 to A.B.-M.).

AUTHOR CONTRIBUTIONS

A.B.-M., F.M.-S., A.I.G., C.M.M., J.A.-I., V.C. and M.B.-C., execution of experiments; J.Y., E.R.-O., J.A., S.B., I.C. and J.I.A., provision of human samples and mutant mice; A.B.-M., F.M.-S., A.I.G., V.C., D.B., J.I.A. and P.P., analysis and interpretation of data; A.B.-M., F.M.-S., V.C., D.B., J.I.A. and P.P., manuscript preparation; and P.P., conception, design and supervision of this study.

COMPETING FINANCIAL INTERESTS

The authors declare no competing financial interests.

1. Dinarello, C.A. Immunological and inflammatory functions of the interleukin-1 family. *Annu. Rev. Immunol.* **27**, 519–550 (2009).
2. Schroder, K. & Tschopp, J. The inflammasomes. *Cell* **140**, 821–832 (2010).
3. Lopez-Castejon, G. & Brough, D. Understanding the mechanism of IL-1β secretion. *Cytokine Growth Factor Rev.* **22**, 189–195 (2011).
4. Dinarello, C.A., Donath, M.Y. & Mandrup-Poulsen, T. Role of IL-1β in type 2 diabetes. *Curr. Opin. Endocrinol. Diabetes Obes.* **17**, 314–321 (2010).
5. Neven, B. *et al.* Molecular basis of the spectral expression of CIAS1 mutations associated with phagocytic cell-mediated autoinflammatory disorders CINCA/NOMID, MWS, and FCU. *Blood* **103**, 2809–2815 (2004).
6. Martinon, F., Pétrilli, V., Mayor, A., Tardivel, A. & Tschopp, J. Gout-associated uric acid crystals activate the NALP3 inflammasome. *Nature* **440**, 237–241 (2006).
7. Duewell, P. *et al.* NLRP3 inflammasomes are required for atherogenesis and activated by cholesterol crystals. *Nature* **464**, 1357–1361 (2010).
8. Cai, X. *et al.* Prion-like polymerization underlies signal transduction in antiviral immune defense and inflammasomeactivation. *Cell* **156**, 1207–1222 (2014).
9. Lu, A. *et al.* Unified polymerization mechanism for the assembly of ASC-dependent inflammasomes. *Cell* **156**, 1193–1206 (2014).
10. Mariathasan, S. *et al.* Cryopyrin activates the inflammasome in response to toxins and ATP. *Nature* **440**, 228–232 (2006).
11. Compan, V. *et al.* Cell volume regulation modulates NLRP3 inflammasome activation. *Immunity* **37**, 487–500 (2012).
12. Halle, A. *et al.* The NALP3 inflammasome is involved in the innate immune response to amyloid-beta. *Nat. Immunol.* **9**, 857–865 (2008).
13. Babelova, A. *et al.* Biglycan, a danger signal that activates the NLRP3 inflammasome via toll-like and P2X receptors. *J. Biol. Chem.* **284**, 24035–24048 (2009).
14. Yazdi, A.S. *et al.* Nanoparticles activate the NLR pyrin domain containing 3 (Nlrp3) inflammasome and cause pulmonary inflammation through release of IL-1α and IL-1β. *Proc. Natl. Acad. Sci. USA* **107**, 19449–19454 (2010).
15. Eisenbarth, S.C., Colegio, O.R., O'Connor, W., Sutterwala, F.S. & Flavell, R.A. Crucial role for the Nalp3 inflammasome in the immunostimulatory properties of aluminium adjuvants. *Nature* **453**, 1122–1126 (2008).
16. Rajamäki, K. *et al.* Extracellular acidosis is a novel danger signal alerting innate immunity via the NLRP3 inflammasome. *J. Biol. Chem.* **288**, 13410–13419 (2013).
17. Hornung, V. *et al.* Silica crystals and aluminum salts activate the NALP3 inflammasome through phagosomal destabilization. *Nat. Immunol.* **9**, 847–856 (2008).
18. Lopez-Castejon, G. *et al.* Deubiquitinases regulate the activity of caspase-1 and interleukin-1β secretion via assembly of the inflammasome. *J. Biol. Chem.* **288**, 2721–2733 (2013).
19. Shimada, K. *et al.* Oxidized mitochondrial DNA activates the NLRP3 inflammasome during apoptosis. *Immunity* **36**, 401–414 (2012).
20. Zhou, R., Tardivel, A., Thorens, B., Choi, I. & Tschopp, J. Thioredoxin-interacting protein links oxidative stress to inflammasome activation. *Nat. Immunol.* **11**, 136–140 (2009).
21. Muñoz-Planillo, R. *et al.* K^+ efflux is the common trigger of NLRP3 inflammasome activation by bacterial toxins and particulate matter. *Immunity* **38**, 1142–1153 (2013).
22. Murakami, T. *et al.* Critical role for calcium mobilization in activation of the NLRP3 inflammasome. *Proc. Natl. Acad. Sci. USA* **109**, 11282–11287 (2012).
23. Lamkanfi, M. *et al.* Inflammasome-dependent release of the alarmin HMGB1 in endotoxemia. *J. Immunol.* **185**, 4385–4392 (2010).
24. Keller, M., Rüegg, A., Werner, S. & Beer, H.-D. Active caspase-1 is a regulator of unconventional protein secretion. *Cell* **132**, 818–831 (2008).
25. Pétrilli, V. *et al.* Activation of the NALP3 inflammasome is triggered by low intracellular potassium concentration. *Cell Death Differ.* **14**, 1583–1589 (2007).
26. Kahlenberg, J.M., Lundberg, K.C., Kertesy, S.B., Qu, Y. & Dubyak, G.R. Potentiation of caspase-1 activation by the P2X7 receptor is dependent on TLR signals and requires NF-κB-driven protein synthesis. *J. Immunol.* **175**, 7611–7622 (2005).
27. Miao, E.A., Rajan, J.V. & Aderem, A. Caspase-1-induced pyroptotic cell death. *Immunol. Rev.* **243**, 206–214 (2011).
28. Masters, S.L., Simon, A., Aksentijevich, I. & Kastner, D.L. Horror autoinflammaticus: the molecular pathophysiology of autoinflammatory disease. *Annu. Rev. Immunol.* **27**, 621–668 (2009).
29. Gross, O. *et al.* Inflammasome activators induce interleukin-1alpha secretion via distinct pathways with differential requirement for the protease function of caspase-1. *Immunity* **36**, 388–400 (2012).
30. Miao, E.A. *et al.* Caspase-1-induced pyroptosis is an innate immune effector mechanism against intracellular bacteria. *Nat. Immunol.* **11**, 1136–1142 (2010).
31. Balci-Peynircioglu, B. *et al.* Expression of ASC in renal tissues of familial mediterranean fever patients with amyloidosis: postulating a role for ASC in AA type amyloid deposition. *Exp. Biol. Med.* (*Maywood*) **233**, 1324–1333 (2008).
32. Shi, C.S. *et al.* Activation of autophagy by inflammatory signals limits IL-1β production by targeting ubiquitinated inflammasomes for destruction. *Nat. Immunol.* **13**, 255–263 (2012).
33. Nakahira, K. *et al.* Autophagy proteins regulate innate immune responses by inhibiting the release of mitochondrial DNA mediated by the NALP3 inflammasome. *Nat. Immunol.* **12**, 222–230 (2011).
34. Dupont, N. *et al.* Autophagy-based unconventional secretory pathway for extracellular delivery of IL-1β. *EMBO J.* **30**, 4701–4711 (2011).
35. Brinkmann, V. *et al.* Neutrophil extracellular traps kill bacteria. *Science* **303**, 1532–1535 (2004).
36. Shmagel, K.V. & Chereshnev, V.A. Molecular bases of immune complex pathology. *Biochemistry* (*Mosc.*) **74**, 469–479 (2009).
37. Kahlenberg, J.M., Carmona-Rivera, C., Smith, C.K. & Kaplan, M.J. Neutrophil extracellular trap-associated protein activation of the NLRP3 inflammasome is enhanced in lupus macrophages. *J. Immunol.* **190**, 1217–1226 (2013).
38. Garcia-Calvo, M. *et al.* Purification and catalytic properties of human caspase family members. *Cell Death Differ.* **6**, 362–369 (1999).
39. Fernandes-Alnemri, T. *et al.* The pyroptosome: a supramolecular assembly of ASC dimers mediating inflammatory cell death via caspase-1 activation. *Cell Death Differ.* **14**, 1590–1604 (2007).
40. Masters, S.L. *et al.* Activation of the NLRP3 inflammasome by islet amyloid polypeptide provides a mechanism for enhanced IL-1β in type 2 diabetes. *Nat. Immunol.* **11**, 897–904 (2010).
41. Tanaka, N. *et al.* High incidence of NLRP3 somatic mosaicism in patients with chronic infantile neurologic, cutaneous, articular syndrome: results of an International Multicenter Collaborative Study. *Arthritis Rheum.* **63**, 3625–3632 (2011).
42. Nakagawa, K. *et al.* Somatic *NLRP3* mosaicism in Muckle-Wells syndrome. A genetic mechanism shared by different phenotypes of cryopyrin-associated periodic syndromes. *Ann. Rheum. Dis.* doi:10.1136/annrheumdis-2013-204361 (10 December 2013).
43. Hoffman, H.M. *et al.* Prevention of cold-associated acute inflammation in familial cold autoinflammatory syndrome by interleukin-1 receptor antagonist. *Lancet* **364**, 1779–1785 (2004).
44. Hoffman, H.M. *et al.* Efficacy and safety of rilonacept (interleukin-1 Trap) in patients with cryopyrin-associated periodic syndromes: results from two sequential placebo-controlled studies. *Arthritis Rheum.* **58**, 2443–2452 (2008).
45. Lachmann, H.J. *et al.* Use of canakinumab in the cryopyrin-associated periodic syndrome. *N. Engl. J. Med.* **360**, 2416–2425 (2009).
46. Adamczak, S. *et al.* Inflammasome proteins in cerebrospinal fluid of brain-injured patients as biomarkers of functional outcome: clinical article. *J. Neurosurg.* **117**, 1119–1125 (2012).

ONLINE METHODS

Animals. Wild-type C57BL/6J mice were from Harlan, *Nlrp3*$^{-/-}$ mice[6], *Pycard*$^{-/-}$ mice[47] and *Casp1*$^{-/-}$*Casp11*$^{-/-}$ mice[48], all on C57BL/6J background, were maintained in specific pathogen–free conditions at a room temperature of 20 ± 2 °C, and a 12-hour/12-hour light/dark cycle. The mice were fed a sterile commercial pellet diet and were provided sterile tap water *ad libitum*. The procedure of peritonitis in mice induced by intraperitoneal injection of particles was approved by the "Servicio de Sanidad Animal, Dirección General de Ganadería y Pesca, Consejería de Agricultura y Agua Región de Murcia" (Health Animal Service, Murcia Fishing and Farming Council) with reference C1310050308. Mice were used at 6–10 weeks of age and were assigned randomly to groups and were given intraperitoneal injection of saline vehicle solution or 4×10^6 ASC-YFP or NLRP3(p.D303N)-YFP recombinant particles, followed by analysis 16 h later. Sample size was estimated according to experience and other similar published work[6]. The researchers were not 'blinded' to sample identity.

Human samples. Whole peripheral blood samples were collected after written informed consent was obtained from healthy donors (n = 8) and from patients with various monogenic inherited autoinflammatory syndromes (n = 28 (cryopyrin-associated periodic syndromes), 6 (Familial Mediterranean Fever) or 6 (TNF receptor–associated periodic syndrome); **Supplementary Table 1**). The serum fraction of these samples was separated by centrifugation at 680*g* for 5 min and was frozen at −80 °C. The Institutional Review Board of Hospital Clinic approved the use these serum samples.

Reagents. LPS from *E. coli* strain O55:B5, DAPI (4,6-diamidino-2-phenylindol), ATP, cytochalasin B, Triton X-100, NAC and nigericin were from Sigma; recombinant caspase-1, the caspase-1 inhibitor Ac-YVAD-AOM and the specific caspase-1 substrate z-YVAD-AFC were from Merk-Millipore; monosodium urate crystals was from Enzo Life Sciences; flagellin from *S. typhimurium* and poly(dA:dT)/LyoVec were from Invivogen; the receptor-binding protein protective antigen and metalloprotease lethal factor were from List Biological; the protein-delivery reagent PULSin was from PolyPlus Transfection; the crosslinking reagent SDA (succinimidyl 2-([4,4′-azipentanamido]ethyl)-1,3′-dithiopropionate; Thermo Scientific); phalloidin-rhodamine and horseradish peroxidase–anti-β-actin (C4; sc-47778HRP), anti-GFP (FL; sc-8334), rabbit polyclonal antibody to caspase-1 p10 (M-20; sc-514), anti-IL-1β (H-153; sc-7884) and anti-ASC ((N-15)-R; sc-22514-R) were from Santa Cruz Biotechnology. Mouse monoclonal anti-NLRP3 (Cryo-2; AG-20B-0014), mouse monoclonal antibody to caspase-1 p20 (Casper-1; AG-20B-0042) and rabbit polyclonal anti-ASC (AL177; AG-25B-0006) were from AdipoGen. Ca074Me was from Merk-Millipore. Secondary antibodies for immunoblot analysis (ECL horseradish peroxidase–conjugated–linked whole sheep antibody to mouse IgG (NA931V) and ECL horseradish peroxidase–conjugated–linked donkey antibody ($F(ab')_2$ fragment) to rabbit IgG (NA9340V)) were from GE Healthcare. Alexa Fluor 488–conjugated donkey antibody to rabbit IgG (heavy and light chain) (A-21206), Alexa Fluor 555–conjugated donkey antibody to mouse IgG (heavy and light chain) (A-31570), Alexa Fluor 555–conjugated donkey antibody to rabbit IgG (heavy and light chain) (A-31572) and cholera toxin B–Alexa Fluor 647 were from Life Technologies.

Cells and treatments. BMDMs were obtained from C57BL/6J or mutant mice as described[11]. HEK293T cells (CRL-11268; American Type Culture Collection) were maintained DMEM:F12 (1:1) supplemented with 10% FCS (FCS), 2 mM Glutamax and 1% penicillin-streptomycin (Life Technologies) and were routinely tested for mycoplasma contamination with a Mycoplasma Detection Kit (Roche). Lipofectamine 2000 was used for the transfection of HEK293 cells according to the manufacturer's instructions (Life Technologies). For stable selection of HEK293 cells, constructs encoding YFP-tagged NLRP3 mutants were generated by overlapping PCR and were cloned into pcDNA3.1/V5-His TOPO (Life Technologies). After sequencing was done to ensure the correct mutations were included, the vectors were transfected as described above, and 2 d later the cell culture medium was supplemented with the aminoglycoside G418 (2 mg/ml; Acros Organic), followed by incubation for 4 weeks. Cells were then cloned for further 4–8 weeks by serial dilution in 96-well plates in the presence of G418, and positive clones were expanded. Immortalized mouse BMDMs from wild-type, *Pycard*$^{-/-}$ or *Nlrp3*$^{-/-}$ mice were a gift from E. Latz and were maintained as described[17]. All macrophages were primed for 4 h with LPS (1 μg/ml) and subsequent NLRP3 activation was achieved for 30 min with ATP (5 mM) or nigericin (20 μM) or for 16 h with monosodium urate crystals (200 μg/ml) or for 1 h with live *E. coli* (multiplicity of infection, 20), followed by the addition of 100 U/ml penicillin-streptomycin and incubation for a further 16 h. Activation of the NLRP1, NLRC4 or AIM2 inflammasome was achieved by treatment for 16 h with anthrax lethal toxin (2.5 μg/ml receptor-binding protein and 1 μg/ml metalloprotease lethal factor mix), flagelin (100 ng recombinant protein mixed with PULSin) or poly(dA:dT) (5 μg/ml of poly(dA:dT)/LyoVec), respectively. ASC-YFP or NLRP3(p.D303N)-YFP recombinant particles were incubated at various ratios of particle to macrophage. After cells were stimulated, cell supernatants were collected, centrifuged at 300*g* for 8 min at 4 °C for elimination of cells detached due to cell death, to generate cell-free medium preparations. Before analysis, proteins in supernatants (soluble and insoluble) were concentrated by centrifugation at 11,200*g* for 30 min at 4 °C through a column with a cut-off of 10 kDa (Microcon; Merk-Millipore). All supernatants were free of genomic DNA, as assessed by absorbance at 260 nm and PCR amplification, and therefore we discarded any contaminating dying cells.

Isolation of particles of recombinant ASC and NLRP3. HEK293 cells transiently expressing ASC-YFP or stably expressing NLRP3(p.D303N)-YFP were used for isolation of inflammasome particles as described[49]. Cells were lysed in buffer A (20 mM HEPES-KOH, pH 7.5, 10 mM KCl, 1.5 mM $MgCl_2$, 1 mM EDTA, 1 mM EGTA and 320 mM sucrose) by passage of the lysate 30 times through a 1-ml syringe with a 25-gauge needle at 4 °C. Cell lysates were centrifuged at 400*g* for 8 min and supernatants was filtered through a 5-μm filter (Millipore). Clarified cell lysates were diluted with one volume of CHAPS buffer (20 mM HEPES-KOH, pH 7.5, 5 mM $MgCl_2$, 0.5 mM EGTA, 0.1 mM PMSF and 0.1% CHAPS), followed by centrifugation, to pellet oligomeric complex structures of ASC or NLRP3(p.D303N), and washing in CHAPS buffer. ASC-YFP and NLRP3(p.D303N)-YFP were then subjected to Percoll gradient centrifugation and then inflammasome particles were separated, washed in CHAPS buffer and quantified by counting of fluorescent particles with a Bürker chamber. ASC-YFP and NLRP3(p.D303N)-YFP particles were then adjusted to a density of 5×10^5 specks per μl. As control, lysate from mock-transfected HEK293 cells were subjected to this protocol and the final product was used as negative control in the experiments.

Immunocytochemistry and fluorescence microscopy. Macrophages stimulated on coverslips were washed twice with PBS, incubated for 10 min with cholera toxin B–Alexa Fluor 647 (1:2,500 dilution) and fixed for 15 min at room temperature with 4% formaldehyde in PBS, and then were washed three times with PBS. Nonspecific binding in cells was blocked with 1% bovine serum albumin (Sigma) and cells were permeabilized for 30 min at room temperature with 0.2% saponin (Fluka) in PBS before incubation for 1 h at room temperature with the primary antibody rabbit anti-ASC (1:200 dilution; (N-15)-R; sc-22514-R; Santa Cruz Biotechnology) or anti-caspase-1 (1:200 dilution; Casper-1; AG-20B-0042; AdipoGen). Cells were washed and then were incubated for 2 h at room temperature with the appropriate fluorescence-conjugated secondary antibody (1:200 dilution; identified above), then were rinsed in PBS and incubated for 20 min with phalloidin-rhodamine (300 nM). All coverslips were mounted on slides with Fluoroshield with DAPI (Sigma).

For nucleation experiments, soluble ASC-mCherry was incubated for 2 h at 37 °C with 5×10^5 ASC-YFP or mutant NLRP3-YFP particles in CHAPS buffer. For the production of soluble ASC-mCherry, unstimulated immortalized ASC-mCherry macrophages were lysed in CHAPS buffer by being syringed 20 times with a 25-gauge needle at 4 °C. Cell lysates were centrifuged at 14,000 r.p.m. for 8 min and clarified cell lysates were then centrifuged at 23,000*g* for 1 h to generate a particulate-free supernatant.

Images were acquired with a Nikon Eclipse Ti microscope equipped with a 20× S Plan Fluor objective (numerical aperture, 0.45), a 40× S Plan Fluor objective (numerical aperture, 0.60) and a 60× Plan Apo Vc objective (numerical aperture, 1.40) and a digital Sight DS-QiMc camera (Nikon) with a Z optical

doi:10.1038/ni.2919

spacing of 0.2 µm and 387-nm/447-nm, 472-nm/520-nm, 543-nm/593-nm and 650-nm/668-nm filter sets (Semrock). Maximum-intensity projection of images was achieved with NIS-Elements AR software (Nikon) and ImageJ software (US National Institutes of Health).

Electron microscopy. Particles of recombinant ASC or NLRP3 and macrophages stimulated in suspension were centrifuged and pellets were fixed for 1.5 h at 4 °C in 2.5% buffered glutaraldehide (Sigma) in 0.1 M cacodilatre buffer. After fixation, pellets were immersed for 8 h in 0.01 M cacodylate buffer solution, then were post-fixed for 2 h in the dark in 1% osmium tetroxide (Sigma) in 0.1 M cacodilate buffer and were counterstained for 2 h with 2% uranyl acetate (Sigma) in Michaelis sodium acetate–sodium veronal buffer. The pellets were then dehydrated in ethanol at an increasing gradient (30%, 50%, 70%, 90% and 100%), were immersed for 15 min in propylene oxide (Sigma) and then were immersed for 16 h in a mixture of propylene oxide and Epon812 resin (1:1 ratio; Tousimis). The solution was then exchanged for pure Epon812 solution, followed by immersion for 3 h. The pellets were then placed in capsules, embedded in fresh Epon812 and incubated for 72 h at 70 °C. Ultrathin sections (40 nm in thickness) were obtained from specimens with a microtome (Leyca microsystems) and were placed onto copper grids (Sigma). Grids were finally post-stained by immersion for 2 h in 2% uranyl acetate in veronal buffer (Lonza) and immersion for 5 min in lead citrate (SPI). Grids were then visualized with a Jeol JEM-1011 transmission electron microscope.

Flow cytometry. For the detection of extracellular particles of ASC and NLRP3, 0.5 ml of human serum or culture supernatants of stimulated macrophages were incubated for 1 h with 1 µg rabbit polyclonal anti-ASC (AL177; AG-25B-0006; AdipoGen) and mouse monoclonal anti-NLRP3 (Cryo-2; AG-20B-0014; AdipoGen). Particles were centrifuged and washed before incubation with the following secondary antibodies: Alexa Fluor 647–conjugated goat antibody ($F(ab')_2$ fragment) to rabbit IgG (heavy and light chain) (A-21246) and R-phycoerythrin–conjugated goat antibody ($F(ab')_2$ fragment) to mouse IgG (heavy and light chain) (A-10543) (both from Life Technologies). Samples were washed before being analyzed by flow cytometry with a FACSCanto (BD Biosciences) and FACSDiva software (BD Biosciences) by gating for small particles or cell debris based on forward scatter versus side scatter, adjusted to display correct separation of leukocyte populations. Gated events are presented on plots showing percent positive particles.

Peritoneal cells from mice given injection of saline vehicle solution or particles of ASC-YFP or NLRP3-YFP were counted and washed and then incubated for 10 min with Mouse SeroBlock FcR (ABD Serotec). Cells were then incubated for 30 min with phycoerythrin-conjugated antibody to mouse Ly6G (anti-Gr-1; RB6-8C5; 12-5931-81; eBioscience) and allophycocyanin-conjugated rat antibody to mouse CD11b (anti-Mac-1; M1/79; 561690; BD Biosciences). Cells were analyzed by flow cytometry with gating of leukocytes on the basis of forward scatter versus side scatter.

Coimmunoprecipitation, ASC oligomerization and immunoblot analysis. Details of the methods used for immunoblot analysis and ASC oligomerization-crosslinking have been reported[11,49]. Immunoblot analysis results were analyzed by densitometry with Quantity One software (BioRad). For coimmunoprecipitation, equal amounts of cell supernatant were incubated for 1 h at 4 °C with 1.5 µg anti-ASC or irrelevant rabbit IgG and then for 1 h at 4 °C with protein G–agarose beads (Merk-Millipore). Beads were washed three times and heated for 5 min at 80 °C with reducing loading sample buffer (Life Technologies). HEK293 cells stably expressing pro-IL-1β–YFP were lysed in cell lysis buffer (25 mM HEPES, pH 7.5, 5 mM $MgCl_2$, 5 mM EDTA and 5 mM DTT) and lysates were incubated for 2 h at 37 °C with 10 U of recombinant caspase-1 or concentrated supernatants from ATP- or nigericin treated macrophages supplemented or not with 50 µM Ac-YVAD-AOM (caspase-1 inhibitor).

ELISA, multiplex flow cytometry and measurement of LDH release, caspase-1 activity and CRP. ELISA kits for human or mouse IL-1β were from R&D Systems. IL-6, IL-1β and TNF in human serum samples was smultaneously analyzed with a Cytometric Bead Array Enhanced Sensitivity 3 Plex Set according to the manufacturer's instructions (BD Biosciences). CRP in serum was measured by the immunoturbidimetric method with a Cobas 6000 and a c501 module (Roche Diagnostics). Extracellular LDH was detected with a Cytotoxicity Detection kit (Roche) and results are present as the percent of the total intracellular LDH. Caspase-1 activity was measured by monitoring of cleavage of the fluorescent substrate z-YVAD-AFC at 400 nm and 505 nm with a Synergy Mx plate reader (BioTek) for 6 h at 30-minute intervals. Results are presented as either the relative fluorescence units (RFU) or 'caspase-1 units' calculated with a standard curve generated with different concentrations of recombinant caspase-1.

Membrane permeabilization. Dye uptake was analyzed with a Synergy Mx plate reader (BioTek), and YOPRO-1 (Life Technologies) bound to DNA fluorescence was measured at an excitation of 485 nm and an emission of 515 nm. Cells were preincubated with 2.5 µM YOPRO-1. The fluorescence signal was recorded for 30 min at intervals of 6 s before and during incubation at 37 °C with ATP (5 mM) or nigericin (20 µM). Maximum fluorescence was obtained by permeabilization of the cells with Triton-X100 (0.1%).

Statistical analysis. Statistics were calculated with Prism software (GraphPad). Given the differences found in the release of cytokines from primed macrophages in our previous work, we chose a sample size that ensured adequate power to detect an effect of a prespecified size. The data allowed evaluation of distribution normality by the Kolmogorov-Smirnov test ($\alpha = 0.05$). For two-group comparisons, a two-tailed unpaired *t*-test was used. Comparisons of multiple groups were analyzed by one-way analysis of variance ANOVA with Bonferroni's multiple-comparison test or Dunnett's test for comparison of all groups with the control group. We found that the variance from the groups compared did not present statistically significant differences.

47. Mariathasan, S. *et al.* Differential activation of the inflammasome by caspase-1 adaptors ASC and Ipaf. *Nature* **430**, 213–218 (2004).
48. Kuida, K. *et al.* Altered cytokine export and apoptosis in mice deficient in interleukin-1 beta converting enzyme. *Science* **267**, 2000–2003 (1995).
49. Fernandes-Alnemri, T. & Alnemri, E.S. Assembly, purification, and assay of the activity of the ASC pyroptosome. *Methods Enzymol.* **442**, 251–270 (2008).